Czech Technical University in Prague

FACULTY OF MECHANICAL ENGINEERING

Department of Production Machines and Equipment

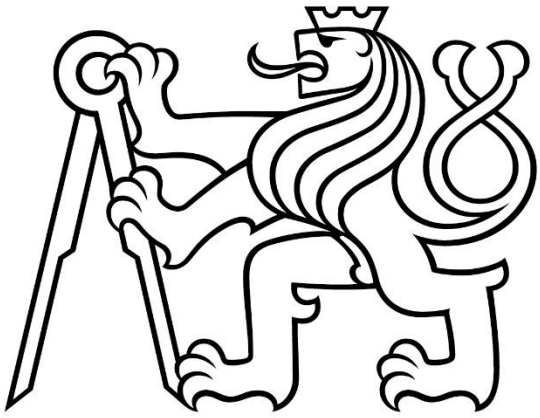

Master's thesis

Influence of input parameters on approximation quality of milling centre thermal error model

2021 **Bc. Michal Straka**

MASTER'S THESIS ASSIGNMENT

I. Personal and study details

Student's name: **Straka Michal** Personal ID number: **466684**

Faculty / Institute: **Faculty of Mechanical Engineering**

Department / Institute: **Department of Production Machines and Equipment**

Study program: **Mechanical Engineering**

Branch of study: **Production Machines and Equipment**

II. Master's thesis details

Master's thesis title in English:

Influence of input parameters on approximation quality of milling centre thermal error model

Master's thesis title in Czech:

Vliv vstupních parametrů na aproximační kvalitu modelu teplotních chyb frézovacího centra

Guidelines:

Topic description: Research of impact of input parameters on approximation quality of thermal error compensation model of milling centre caused by movement in linear axes. Application of the model on other machines of the same production line. Model transferability analyses; Work syllabus: 1. State of the art. 2. Experimental work, data processing and interpretation. 3. Model calibration. 4. Model application on data from other machines of the same production line. 5. Model modification and effort analyse; Scope of the graphic part: without drawing documentation; Range of the text part: 60-80 pages;

Bibliography / sources:

[1] J. Mayr, et al., "Thermal issues in machine tools," CIRP Annals – Man. Tech., Vol.61, No.2, pp. 771-791, 2012.; [2] O. Horejš, et al., "A general approach to thermal error modelling of machine tools", In: Machines et usinage à grande vitesse (MUGV), Clermont Ferrand, France. 2014.; [3] M. Mareš, et al., "Thermal error compensation of a 5-axis machine tool using indigenous temperature sensors and CNC integra-ted Python code validated with a machined test piece", In: Precision Engineering 66, 2020, s. 21-30.;

Name and workplace of master's thesis supervisor:

Ing. Martin Mareš, Ph.D., Department of Production Machines and Equipment, FME

Name and workplace of second master's thesis supervisor or consultant:

Ing. Otakar Horejš, Ph.D., Department of Production Machines and Equipment, FME

Date of master's thesis assignment: **29.04.2021** Deadline for master's thesis submission: **25.07.2021**

Assignment valid until: **30.09.2021**

Ing. Martin Mareš, Ph.D. Supervisor's signature	Ing. Matěj Sulitka, Ph.D. Head of department's signature	prof. Ing. Michael Valášek, DrSc. Dean's signature

III. Assignment receipt

The student acknowledges that the master's thesis is an individual work. The student must produce his thesis without the assistance of others, with the exception of provided consultations. Within the master's thesis, the author must state the names of consultants and include a list of references.

Date of assignment receipt	Student's signature

ZADÁNÍ DIPLOMOVÉ PRÁCE

I. OSOBNÍ A STUDIJNÍ ÚDAJE

Příjmení: **Straka** Jméno: **Michal** Osobní číslo: **466684**

Fakulta/ústav: **Fakulta strojní**

Zadávající katedra/ústav: **Ústav výrobních strojů a zařízení**

Studijní program: **Strojní inženýrství**

Studijní obor: **Výrobní stroje a zařízení**

II. ÚDAJE K DIPLOMOVÉ PRÁCI

Název diplomové práce:

Vliv vstupních parametrů na aproximační kvalitu modelu teplotních chyb frézovacího centra

Název diplomové práce anglicky:

Influence of input parameters on approximation quality of milling centre thermal error model

Pokyny pro vypracování:

Popis tématu: Výzkum vlivu možných vstupních parametrů (teplot) na aproximační kvalitu modelu teplotních chyb frézovacího centra způsobených především pohybem lineárních os. Návrh modelu. Aplikace modelu na data z dalších strojů stejné produktové řady. Analýza náročnosti přenositelnosti modelu; Osnova práce: 1. Rešerše metod pro minimalizaci teplotních deformací obráběcích strojů s ohledem na praktické použití. 2. Realizace experimentů, zpracování a interpretace naměřených dat. 3. Rozvaha nad možnostmi kalibrace aproximačních modelů. Sestavení modelů. 4. Aplikace sestavených modelů na jiné stroje stejného typu. 5. Modifikace kompenzačních modelů a analýza náročnosti modifikace.; Rozsah grafické části: bez výkresové dokumentace; Rozsah textové části: 60-80 stran;

Seznam doporučené literatury:

[1] J. Mayr, et al., "Thermal issues in machine tools," CIRP Annals – Man. Tech., Vol.61, No.2, pp. 771-791, 2012.; [2] O. Horejš, et al., "A general approach to thermal error modelling of machine tools", In: Machines et usinage à grande vitesse (MUGV), Clermont Ferrand, France. 2014.; [3] M. Mareš, et al., "Thermal error compensation of a 5-axis machine tool using indigenous temperature sensors and CNC integra-ted Python code validated with a machined test piece", In: Precision Engineering 66, 2020, s. 21-30.;

Jméno a pracoviště vedoucí(ho) diplomové práce:

Ing. Martin Mareš, Ph.D., ústav výrobních strojů a zařízení FS

Jméno a pracoviště druhé(ho) vedoucí(ho) nebo konzultanta(ky) diplomové práce:

Ing. Otakar Horejš, Ph.D., ústav výrobních strojů a zařízení FS

Datum zadání diplomové práce: **29.04.2021** Termín odevzdání diplomové práce: **25.07.2021**

Platnost zadání diplomové práce: **30.09.2021**

Ing. Martin Mareš, Ph.D. podpis vedoucí(ho) práce	Ing. Matěj Sulitka, Ph.D. podpis vedoucí(ho) ústavu/katedry	prof. Ing. Michael Valášek, DrSc. podpis děkana(ky)

III. PŘEVZETÍ ZADÁNÍ

Diplomant bere na vědomí, že je povinen vypracovat diplomovou práci samostatně, bez cizí pomoci, s výjimkou poskytnutých konzultací. Seznam použité literatury, jiných pramenů a jmen konzultantů je třeba uvést v diplomové práci.

.	
Datum převzetí zadání	Podpis studenta

Statement

I declare that my thesis was developed independently and that all used information sources are stated in enclosed list in accordance with the Guidelines of adhering to ethical principles in the preparation of undergraduate theses, issued by the Czech Technical University in Prague on 1/7 2009.

I do not have a relevant reason against the use of this school work in accordance with § 60 of the Act no.121 / 2000 Sb., on copyright, rights related to copyright and amending some laws (Copyright Act).

In Prague on 25.7.2021 ……..…….

signature

Acknowledgement

I would like to express my sincere thanks to my supervisor, Ing. Martin Mareš, Ph.D., for responsible guidance and a lot of valuable feedback. I would like to thank my consultant, Ing. Otakar Horejš, Ph.D., for his help and support. Also, thank you to my family for their patience and encouragement during my studies. Finally, I would like to thank my girlfriend, Mgr. Hana Krátká, for all her love, help, and support.

The results of the work were applied to an article in the impact journal.

HSM 2021

MM Science Journal | www.mmscience.eu
ISSN 1803-1269 (Print) | ISSN 1805-0476 (Online)
Special Issue | HSM 2021
16th International Conference on High Speed Machining
October 26-27, 2021, Darmstadt, Germany
DOI: XXXXXX

MM SCIENCE JOURNAL

HSM2021-00000

THE IMPACT OF KEY TEMPERATURE MEASURING POINTS ON THERMAL ERROR COMPENSATION MODEL TRANSFER BETWEEN MILLING CENTERS OF THE SAME PRODUCT LINE

M. Straka[1], M. Mareš[1]*, O. Horejš[1]

[1] Czech Technical University in Prague, Faculty of Mechanical Engineering, Department of Production Machines and Equipment, RCMT, Horská 3, 128 00 Prague, Czech Republic

*Corresponding author; e-mail: m.mares@rcmt.cvut.cz

Toto téma diplomové práce je podpořené projektem "Strojírenská výrobní technika a přesné strojírenství" CZ.02.1.01./0.0/0.0/16_026/0008404 prostřednictvím Operačního programu Výzkum, vývoj, vzdělávání (poskytovatel MŠMT ČR) a spolufinancován Evropskou unií.

This thesis is supported by the project "Mechanical Engineering Production Technology and Precision Engineering" CZ.02.1.01./0.0/0.0/16_026/0008404 through the Operational Programme: Research, Development, Education (provided by the Ministry of Education, Youth and Sports of the Czech Republic) and co-financed by the European Union.

Annotation

Author:	Michal Straka
Title of master thesis:	Influence of input parameters on approximation quality of milling centre thermal error model
Extent:	83 p., 38 fig., 13 tab.
Academic year:	2021
University:	CTU in Prague, Faculty of Mechanical Engineering
Department:	Ú12135 – Department of Production Machines and Equipment
Supervisor:	Ing. Martin Mareš, Ph.D.
Consultant:	Ing. Otakar Horejš, Ph.D.
Submitter of the Theme:	CTU in Prague, Faculty of Mechanical Engineering
Application:	Evaluation of the influence of different input parameters on the approximation quality and portability evaluation of thermal compensation models.
Key words:	thermal error, compensation, machine tool, key temperature input, portability
Annotation:	The thesis is focused on evaluating the influence of different input parameters (temperatures) into the compensation models of thermal errors caused by movement in the linear axes of the machine tool. The portability of thermal error compensation models among multiple machine tools of similar structure and size was evaluated.

Anotace

Autor:	Michal Straka
Název diplomové práce:	Vliv vstupních parametrů na aproximační kvalitu modelu teplotních chyb frézovacího centra
Rozsah práce:	83 str., 38 obr., 13 tab.
Školní rok vyhotovení:	2021
Škola:	ČVUT v Praze, Fakulta Strojní
Ústav:	Ú12135 – Ústav výrobních strojů a zařízení
Vedoucí bakalářské práce:	Ing. Martin Mareš, Ph.D.
Konzultant:	Ing. Otakar Horejš, Ph.D.
Zadavatel:	ČVUT v Praze, Fakulta Strojní
Využití:	Posouzení vlivu různých vstupních parametrů na aproximační kvalitu a hodnocení přenositelnosti teplotních kompenzačních modelů.
Klíčová slova:	teplotní chyba, kompenzace, výrobní stroj, klíčový teplotní vstup, přenositelnost
Anotace:	Diplomová práce se zabývá posouzením vlivu různých vstupních parametrů (teplot) do kompenzačních modelů teplotních chyb způsobených pohybem v lineárních osách výrobního stroje. Byla hodnocena přenositelnost kompenzačních modelů teplotních chyb mezi více stroji podobné konstrukce a velikosti.

Content

Nomenclature

amb	ambient
AMP	another machine producer
ANN	artificial neural network
ARX	Autoregressive model with external input
a_n	calibration coefficient of the transfer function input [µm^2/°C]
b_m	calibration coefficient of the transfer function output [µm]
C	corrected thermal compensation model
c_p	specific heat capacity [J·kg^{-1}·K^{-1}]
dyn	dynamic
E	excitation of a dynamic system [K]
ETVE	environmental temperature variation error
FDM	finite difference method
FEM	finite element method
FIT	global indicator of approximation quality [%]
g	correction factor
in	input source of thermal compensation model (temperature sensor)
l	length of the MT part [um]
l_1	the default length of the MT part [um]

LTI	Linear Time Invariant
mea	measured
MLRA	Multiple linear regression analysis
MT	machine tool
N	uncorrected thermal compensation model
OE	Output error model
PTP	peak-to-peak method; the worst absolute approximation quality
R	response of a dynamic system [µm]
RCMT	Research Center of Manufacturing Technology
RES	residuum; a local indicator of approximation quality [µm]
S/N	serial number
stat	static
syst	system
TCP	tool centre point
T_{in}	input in thermal compensation model [K]
$T_{Y,Z\ dyn}$	sensor on the front side of the ball screw nut in Y, Z direction
$T_{Y,Z\ stat}$	sensor on bearing house of the bearing screw in Y, Z direction
$T_{Y,Z\ syst}$	sensor in the motor of linear axis Y, Z
$u(t)$	the input of the system in the time domain
XTY	deformation in X machine direction during linear motion in Y-axis [um]

XTZ	deformation in X machine direction during linear motion in Z-axis [um]
Y	input data matrix (temperature, spindle speed, etc.)
$y(t)$	the output of the system in the time domain
YTY	deformation in Y machine direction during linear motion in Y-axis [um]
YTZ	deformation in Y machine direction during linear motion in Z-axis [um]
ZTY	deformation in Z machine direction during linear motion in Y-axis [um]
ZTZ	deformation in Z machine direction during linear motion in Z-axis [um]
α	coefficient of thermal expansion [K^{-1}]
β	correction coefficient
δ	thermal error of the e.g. spindle in a definite direction [µm]
δX	deformation at TCP in X direction [µm]
δY	deformation at TCP in Y direction [µm]
δZ	deformation at TCP in Z direction [µm]
ΔT	difference of the (measured) temperature [K]
$\overline{\delta Z}$	arithmetic mean at the time of the measured deformation
ε	transfer function in the time domain [1]
$\varepsilon_{\mathrm{amb}}$	transfer function of ambient environment influence [1]
ε_{in}^{XTY}	transfer function of relevant source (input; in) and deformation (XTY,…,ZTZ) [1]
λ	thermal conductivity coefficient [$W \cdot m^{-1} \cdot K^{-1}$]

1 Motivation

The general motivation of the research is to improve the machine tool (MT) accuracy by using methods to minimize its thermal errors.

The motivation of this thesis is the analysis of different temperature inputs to the compensation model that could have a significant impact on the quality of thermal errors prediction.

Further motivation is the study of the possibilities of an industrial application of thermal compensation models: significant time and resource savings for MT producers could be achieved through model portability. The portability of thermal compensation models could lead to wider adoption of software compensation in their products.

2 Introduction

One of the primary factors influencing the geometric accuracy of MTs are thermal errors [1]. Except for the spindle unit, other elements significantly influencing the thermal behaviour of MT are motors of MT linear axes, movement mechanisms (bearings, lead screws, etc.), and changes in environmental temperature. One approach how to compensate MT thermal error is the use of transfer function [2]. The advantage of models based on transfer functions is a possibility to solve each heat source influence contributing to overall MT thermal error separately. The resulting approximation is then the sum of the solutions of the partial influences (single motors of MT linear axes, lead screws, ball screw nuts, environment, etc.). The input into the transfer function is the temperature in this case. The location where the temperature is measured could significantly influence the approximation quality of the predicted thermal error. Therefore, the influences of using 3 different inputs to the thermal compensation model on the approximation quality of the predicted thermal error were compared. For this purpose, thermal error compensation models based on the transfer function principle were calibrated. The measurements were performed on a 5-axis milling center of the upper gantry type.

The portability of the thermal compensation models to MTs of similar structure and size was further evaluated. The evaluation was performed for 4 MTs of the same product line and one MT by another producer. Results of portability within target machines and thermal compensation models, possible causes of inaccuracies, and impacts on MT producers are discussed in detail.

3 The state of the art

3.1 Deformation of machine tools

The machining accuracy of MTs, resulting in an inaccuracy of dimensions of a machined workpiece, is affected by a number of influences, which can be modified. Very important are the influences of the MT itself, which affect the accuracy of machining.

A MT can generally be considered as a rigid system. However, if the MT is in the working process, it is loaded by many dynamic and non-stationary influences that cause its deformation.

3.1.1 Deformations caused by MT geometry and kinematics

Geometric errors in the MT can occur as a result of inaccuracies in assembly or by choice of an inappropriate construction design. The suitability and quality of the components is also important. Errors can be greatly increased by MT overload.

Kinematic errors are mainly a consequence of linear or circular interpolations and the combined movement of several MT motion axes [3].

3.1.2 Static deformation

Static deformation is related to the static stiffness of MT and its structure, including also deformation errors between the tool and the workpiece. This includes deformations caused by wear of MT, tool or jig components, tool clamping, incorrect jig setting, low tool or jig stiffness, workpiece displacement during the machining, or due to the action of the MT own wight [3].

3.1.3 Dynamic deformation

Dynamic deformations occur during the cutting process. Their size is influenced by the dynamic stiffness of the MT itself (especially the base, stand, etc.), but mainly by the selected cutting conditions. Their inappropriate choice causes vibrations. The accuracy of the MT varies depending on the dynamic stiffness of the structure within the specific cutting conditions.[3].

3.1.4 Thermal deformation

Thermal deformations are caused by the effects of temperature on the MT, and therefore by a longitudinal expansion of the material due to temperature changes [4]. Thermal errors can cause up to 70% of overall MT errors [5]. In detail in section 2.2.

3.2 Heat and thermal deformation in MTs

Change in the temperature *ΔT* in the MT space and its parts *(*ΔT) results from heat-sharing processes in the MT system and its surroundings. It causes a change in the length of the body *l*; see equation (1).

$$l = l_1 \cdot (1 + \alpha \cdot \Delta T) \quad (1)$$

3.2.1 Heat generation in the MT and its transfer

The MT is a complex system with many components that represent heat sources. It is also necessary to consider the thermal influence of the surrounding environment. Heat sources can be divided into two basic groups: internal and external heat sources [6].

- **Internal sources**

In general, spindles and motion axes (motors, bearings, ball screws, linear guides, clutches, etc.) are considered as dominant heat sources in the MT [7]. An

important source of heat generation is also the machining process itself. Most mechanical energy needing to separate chips is converted into heat during the machining process (about 60% of the heat is stored in the chips) [8].

A combination of internal and external heat sources occurs during a real working process. Internal heat sources affect the surrounding air and distribute heat to more distant parts of structures and relatively quickly affect the thermo-mechanical state of the MT structure [6].

- **External sources**

Nearby located machines, aggregates, heaters, lights, direct sunlight, etc., are considered external heat sources affecting MT structure. An important factor is the influence of the ambient air, which can heat or cool the MT due to the difference between the value of the ambient air temperature and the temperature of individual parts of the MT. The change in the ambient temperature of the MT is influenced, e.g., by the opening and closing of gates and windows in the production hall, as well as the geographical location of the MT [6]. The importance is also confirmed by the fact that ambient temperature influences are part of the tests called ETVE (environmental temperature variation error) in the international standard ISO 230-3 [10].

The ambient temperature of the MT changes during the day and during different year seasons in the non-air-conditioned production hall. The change in the ambient temperature of the MT affects both the MT structure and the dimensions of the workpiece. The ambient temperature varies over time but may also variate at different height layers (especially for large MTs) [6].

Heat transfer

A temperature difference causes heat transfer. Heat transfer is always produced from a region of high temperature to another area of lower temperature

(as described in the second law of thermodynamics) in three basic modes (see Fig. 1) [11]:

- Conduction – heat transfer occurs across the medium when a temperature gradient exists in a stationary medium (which may be solid or fluid).
- Convection – heat transfer that will occur between a surface and a moving fluid when they are at different temperatures.
- Radiation – heat transfer by electromagnetic waves between two surfaces at different temperatures.

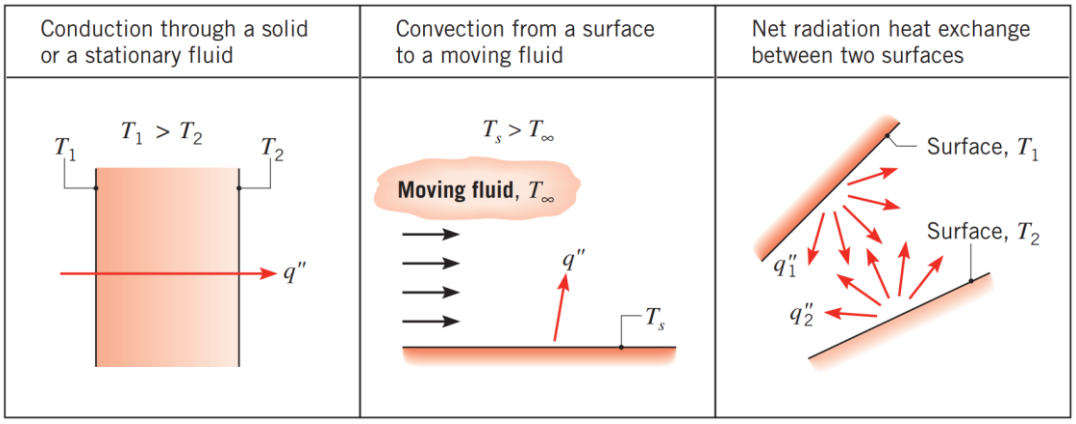

Fig. 1 Conduction, convection, and radiation heat transfer modes [8].

In MT and its modelling, the primary observed influence of heat transfer is conduction in the construction and heat transfer by convection. Heat transfer generated by radiation can usually be considered insignificant inside the MT [12]. However, heat transfer by radiation is relevant in MT, especially in parts reaching high temperatures of more than 450K [13] (e.g., the influence of the cutting process – heat transfer by radiation to the MT structure from hot chips or tools).

It is necessary to create for MT a suitable – ideally a temperature-stable environment without drafts and direct sunlight. The MTs are often placed in air-conditioned rooms if requirements for machining accuracy are very high. However, it is still important, e.g., to prevent the door from opening in the finishing phase of the

machining of precision parts; or to provide full functionality and maximum possible efficiency of the transition chambers at the entrances and exits from the production room.

3.2.2 Thermo-mechanical error

A thermo-mechanical error can be described as a deviation from the planned mutual movement of the tool and the workpiece, which was caused by temperature changes. It is an undesirable relative movement between the tool and the workpiece due to the thermal expansion of the individual parts of the MT [14]. Fig. 2 shows the direct dependence of the temperature error at a TCP of the MT on the temperature field, directly related to the heat sources [15].

Fig. 2 Thermo-elastic functional chain [15].

There are many different heat sources in MT, e.g., motors, pumps, bearings, drives, clutches, gears, guideways, cutting process, chips, external heat sources etc. [14]. The effect of these sources is shown in Fig. 3. The diagram divides the overall thermal problem into two major categories – the impact of uniform temperatures other than 20°C and the effects of non-uniform temperatures [5].

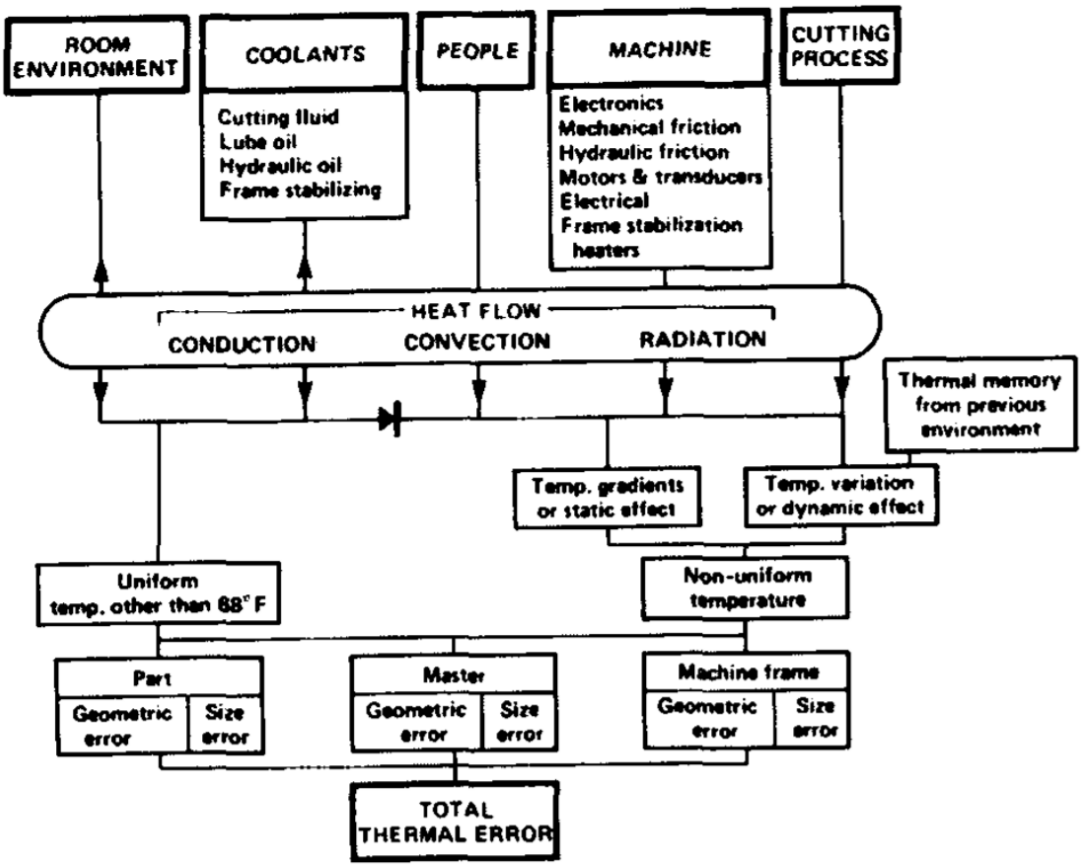

Fig. 3 Diagram of thermal effects on MT [5].

The machining accuracy of the MT is given by the volumetric error of the MT – a combination of all MT errors (geometric, kinematic, static, dynamic, thermal) [16]. Currently, thermal errors are considered to be the most dominant part in the volumetric accuracy of the MT [1]. Thermal errors contribute 40-70% to the total MT error caused within machining [5]; similar conclusions also are in [6]. An extensive survey was attended by 55 manufacturers from Europe and Asia and 20 MT users from Germany in 2018. They were asked about the relevance, causes, and consideration of thermal errors [17]. The results are shown in Fig. 4.

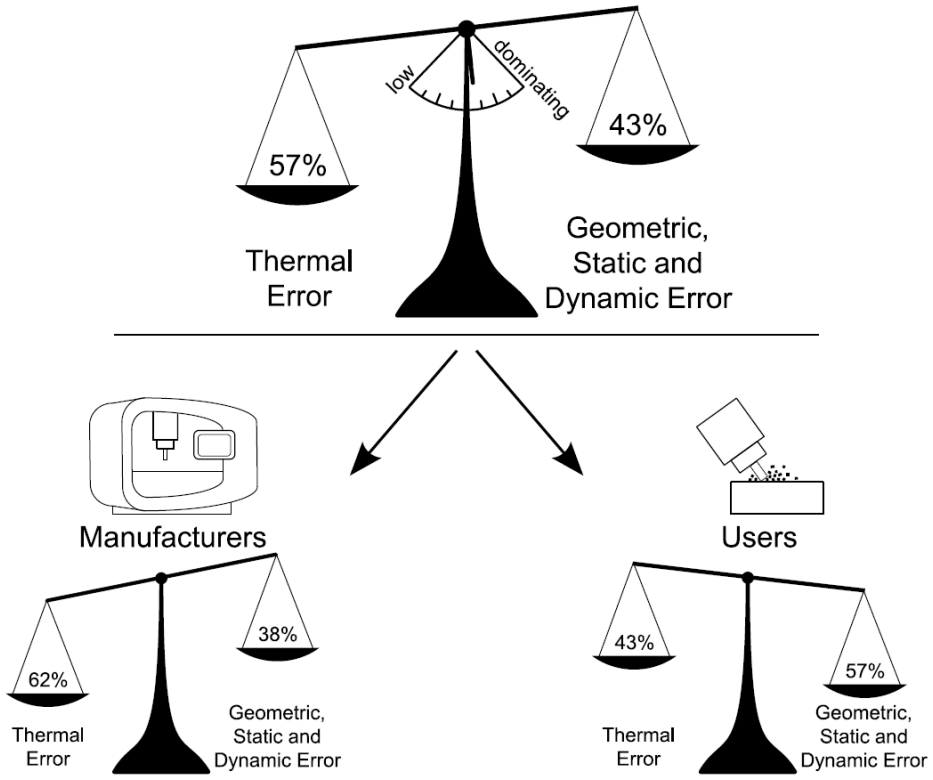

Fig. 4 Assessing the size of the thermal error compared to the total error for all companies [17].

Errors caused by thermal deformation are either geometrical or size (linear). Squareness, straightness, flatness, and angular motion geometrical errors are caused by temperature gradients or non-uniform coefficients of expansion [5]. A simple schema explaining the linear and geometrical thermal deformation can be seen in Fig. 5.

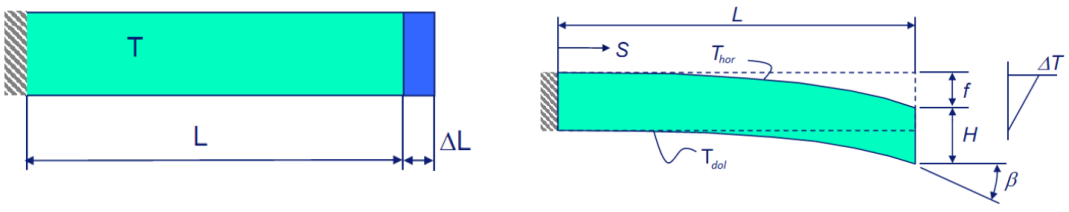

Fig. 5 Schema of the linear and geometrical thermal deformation [18].

The resulting deviations at the TCP are given by several other parameters, such as geometric and kinematic construction of the MT, type of materials used in the construction, etc. The individual parts of the chain of causes and consequences

characterizing the thermal behaviour of the MT are discussed in the next section in more detail.

3.3 Minimization of thermo-mechanical errors of MTs

Thermo-mechanical errors of MT can be reduced by an appropriate choice of the MT structure design, materials used, suitable parts used, or additional cooling at proper locations within the MT.

Methods to reduce thermal errors can be classified into three categories [19]:

- reduction of changes in the temperature field of the MT
- reduction of the MT's sensitivity to changes in the temperature field
- compensation of the thermal errors

3.3.1 Reduction of changes in the temperature field of the MT

There are several ways to reduce changes in the MT's temperature field. The aim is to reduce the heat generated by internal and external heat sources. Possible solutions are described below.

Influence of placement of individual MT parts on heat generation

A MT with a high requirement for machining accuracy should have heat sources (motors, friction clutches, brakes, electric devices, etc.) located as far as possible from MT parts whose thermal expansion directly impacts the relative position between the tool and the workpiece. It is best to place the heat sources completely outside the closed structure of the MT – especially the motors. It is necessary to provide cooling to the heat sources – cooler or free air access. Hydraulic units and electrical devices have to be located outside the MT. It is recommended to replace plain bearings with rolling bearings (rolling resistance is significantly less than shear resistance), and it is necessary to use correct beating lubrication [8].

Temperature control by cooling

- **Fluidic tempering of MT frames**

The MT, equipped with fluidic tempering of MT frames technology, has cooling inserted directly into its supporting structure. The heat generated from the heat sources is immediately and very quickly distributed to other parts of the MT, and it supports warm-up balance. Due to the use of a large amount of coolant, the negative effect of the operating cycle of the cooling unit is significantly eliminated. The big disadvantage of this solution is its technical complexity and high operating costs. [20, 21].

- **Local cooling**

Local cooling is used in areas of significant heat sources, thus mainly for spindles, bearings, axes of movement, ball screws, their nuts, and housings. The cooling medium is most often directly discharged from where the heat source is acting into the external cooling system [20].

Methods applied by the user of the MT

- **Warm up cycle of MT**

A warm-up cycle should be performed before further machining, especially after a longer period of inactivity of the MT. During this process, the MT heats itself to the operating temperature without machining - a state of thermal balance is reached. One of the largest sources of heat in the MT is the spindle unit; therefore, it is almost always heated with the help of the warm-up process by gradually increasing its idle speed.

- **Regulation of the ambient temperature in the production hall**

The influence of the surrounding is in specified geographical conditions (under standard conditions) significant. These do not only change within seasons, months,

or days but literally also during individual work shifts when the temperature in the production hall can change in the order of many degrees during the day. This has a negative impact on the quality, accuracy, and repeatability of production during the day [6].

It is essential to avoid the MT from direct sunlight, temperature influences by other machines standing nearby, and drafts.

It is appropriate to place the MT in an air-conditioned room (or hall) with a constant temperature independent of the surrounding environment if there is a high requirement for machining accuracy. This measure caused higher technological discipline and affected investment, operating, and production costs [20].

- **Reduction of the temperature at the cutting point by cutting fluid**

The MT operator can reduce heat generation (and thus thermal deformation), especially by using local cooling at the cutting point. The cutting fluid lowers the temperature at the cutting point, cools, and helps to remove hot chips, and lowers the temperature of the tool, workpiece, and (partly) the MT. Heat generation can also be reduced by an appropriate choice of technology, cutting conditions, and tools. The resulting machining accuracy is also affected by the temperature of the semi-finished product before machining – it is possible to reduce the resulting size of the machining thermal error by tempering the semi-finished product to the ambient temperature of the MT before machining.

3.3.2 Reducing the sensitivity of the MT to changes in the temperature field

The methods described in the previous section only reduce changes in the temperature field of the MT, which causes a reduction in the thermal error. However, in technical practice, it is almost impossible to eliminate changes in the temperature

field completely. This section focuses on reducing the sensitivity of the MT to changes in the temperature field and thus reducing the generating temperature deformation.

Type of used MT structure

Even during the initial phase of MT construction, the thermo-mechanical behaviour of the MT can be significantly improved. The construction of the MT should be ideally structurally closed and geometrically symmetrical because, in such a construction, the heat is distributed equally. From the point of view of a symmetrical thermo-mechanical structure on both sides of the frame and its closure, the most appropriate is the use of a portal construction (example in Fig. 6 on the left) or a gantry construction. Internal heat sources should also be placed symmetrically within the structure. By their suitable location, thermal deformations can be directed against each other and thus largely eliminated. In using the concept of open construction of the MT (example in the right part of Fig. 6), there is a much more significant proportion of angular thermal deformations, which are less predictable and difficult to compensate only by software tools [20, 22].

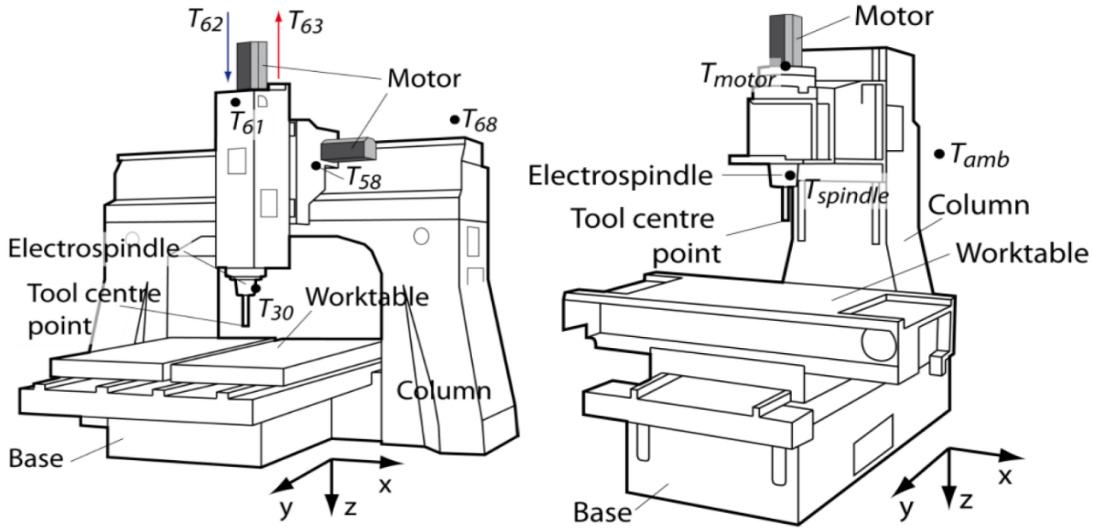

Fig. 6 Example of closed (left) and open construction of MT [20].

Larger parts of the MT (whose thermal deformations could affect the relative position between the tool and the workpiece, e.g., base and columns) should be

arranged to allow chips to escape freely from the tool to distant locations to eliminate the absorption from the removing material. [8].

Another possibility to reduce the sensitivity of the MT to changes in the temperature field in the design phase is the use of topological optimization. The process of topological optimization simply looks for the ideal distribution of construction material in a defined confined space while respecting the specified optimization criteria. In the case of thermo-mechanical topological optimization, the target is to reduce the sensitivity of the MT to changes in the temperature field. Topological optimization is often geometrically very complex structures, which are very difficult (often impossible) to produce by conventional production methods. Moreover, the prevention of other MT properties from deterioration is necessary. It leads to pareto optimisation issues. Therefore, this method is difficult to apply in practice. However, with the development of additive technologies, topological optimization of the thermal behaviour of MT will probably become more important in the near future [23].

It is also possible to optimize the design of the MT with regard to the reduction of thermal deformation by comparing several different design variants of the MT using FEM analysis. As a result, it is possible to determine how much the specified part of the MT contributes to the total thermal deformation [24].

Type of construction material

The choice of construction material has a significant influence not only on the thermal properties of the MT but also on the static and dynamic stiffness of the MT, moments of inertia, the total weight of moving masses, etc. Due to the good weight to stiffness ratio and relatively low purchasing costs, the most used materials for MT construction are steel and cast iron. The disadvantage of these materials is the high value of the coefficient of thermal expansion α. When selecting an appropriate material in terms of thermal behaviour, it is necessary to consider specific heat capacity and thermal conductivity coefficient [20, 22].

- **Coefficient of thermal expansion** - a high value of the parameter α [K^{-1}] has a very negative effect on the geometric accuracy of the MT in terms of thermal deformation. Low α materials are usually more expensive than conventional materials used in MT building (steel, cast iron).
- **Specific heat capacity** - a high value of the parameter c_P [$J \cdot kg^{-1} \cdot K^{-1}$] causes greater temperature stability against changes in ambient temperature. However, it takes a long time for the MT to return to thermal balance after the start of machining – a compromise is needed.
- **Thermal conductivity coefficient** – the high value of the parameter λ [$W \cdot m^{-1} \cdot K^{-1}$] ensures fast homogenization of the internal temperature field of the MT (eliminates asymmetric deformations of the MT if selecting an appropriate construction). However, undesired heating of the entire MT structure from internal heat sources is occurring. Again, a compromise is necessary; with a low parameter λ, local heat concentrations occur at the location of the internal heat source.

Due to their high coefficient of thermal expansion, conventional materials (steel, cast iron) are not very appropriate for the construction of thermally stable and precise MTs. For such MTs are appropriate materials such as granite, polymer concrete, natural granite, fibre composites, or sandwich structures with regard to a positive impact on thermoelasticity. However, these materials usually have a higher purchase price and lower stiffness [20, 22].

Type of position measuring used and its location

The location of the ruler for direct measurement of the position of the MT is important. If the ruler is placed near a heat source, it deforms due to the temperature gradient, which causes the change of positioning accuracy. It is necessary to pay

attention to the location of the direct measuring ruler during the design phase of the MT. The advantage of direct measurement is including thermal deformations of the MT drive (e.g., deformation of ball screws).

3.3.3 Compensation of thermal errors

Another way to eliminate the effect of thermal deformations is by employing compensation methods. More details are in the next section.

3.4 Compensation methods of thermal errors

It is possible to reduce the size of the MT's thermal errors using methods of software compensation of thermal errors. The process of software compensation of thermal errors can be summarised in the following points [25]:

- **Identification** – analysis of MT structure, the definition of appearing types of thermal errors, identification of an appropriate position for measurement sensors, measurements of particular component errors in various operating conditions, assessment of volume errors or maps of geometric volume errors.
- **Error modelling and estimation** – elaboration of component error models, the inclusion of single error models into a complex MT error model, development of error maps, numerical estimation of error values in operational conditions.
- **Prediction and compensation** – installation of an error compensation system, implementation of compensation algorithms or error map to the control system.

Creating an accurate and fast complex numerical thermo-mechanical compensation model is difficult, often almost impossible. During creating such a thermal compensation model, it is necessary to include the MT itself and its interaction with the environment and the influence of the cutting process. Due to the

complexity, several experimental and mathematical methods for determining the generated thermal deformations at TCP were created. It is possible to compensate thermal errors of MT in real-time by using these methods. Based on the form of determining the thermal error, the compensation methods are divided into the following basic groups [6]:

- **Direct methods**

  The size of the thermal deformation is determined by measuring using a laser beam source device or special measurement probes. Then, based on the detected value, the compensation is implemented into the MT control system. This is a fast, accurate, and straightforward way to compensate for thermal errors of MT. The installed equipment can also be used, e.g., to check the tool for wear or damage. The disadvantage is the need to stop the work process during the measurement, the high cost of measuring devices, and the possibility of mainly compensating only the linear part of thermal errors.

- **Indirect methods**

  The values from the calibration measurements are converted to the values required for compensation by using approximation mathematical models, and these results are then implemented into the control system of the MT. It is possible to compensate for both parts of thermal errors (linear, angular). The disadvantage is that it is difficult to separate the thermal deformations from the other deformations of the MT. It is necessary to perform many calibration and verification experiments on the MT set to create a mathematical model that would be as close as possible to the real MT thermal behaviour.

The basic principle of both groups of thermal compensation methods is shown in Fig. 7.

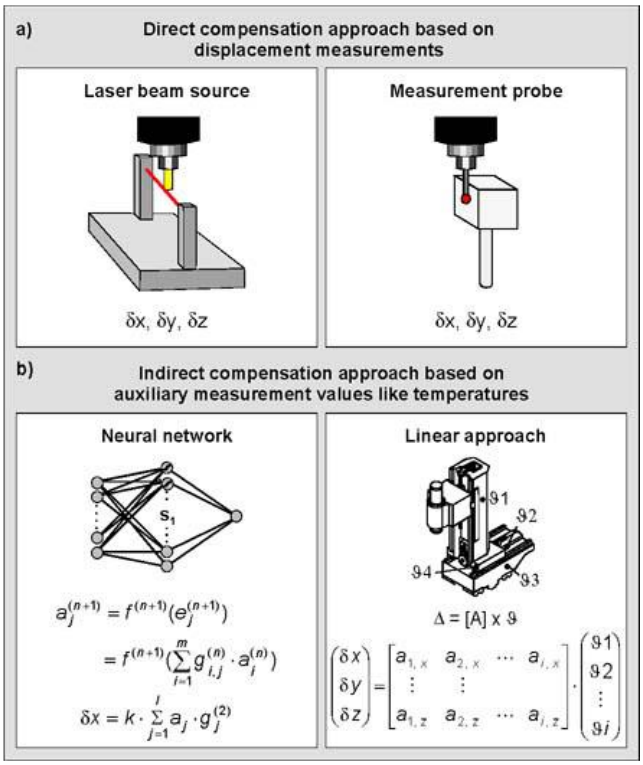

Fig. 7 Common compensation strategies [26].

Software thermal compensations work with a mathematical model which predicts temperature deformation at TCP, based on the measurement of indirect quantities (temperatures, powers, electric currents, etc.). Software thermal compensations are usually created based on experimental data obtained from measurements on a set MT (usually called calibration measurements). The output of the empirically constructed thermal compensation model is the size of thermal errors at TCP, mostly in the directions of the MT coordinate system (X, Y, Z). The occurring errors are then compensated by moving the NC-axes in the opposite direction of the arising deformations [27]. A fundamental principle of the indirect compensation method is shown in Fig. 8.

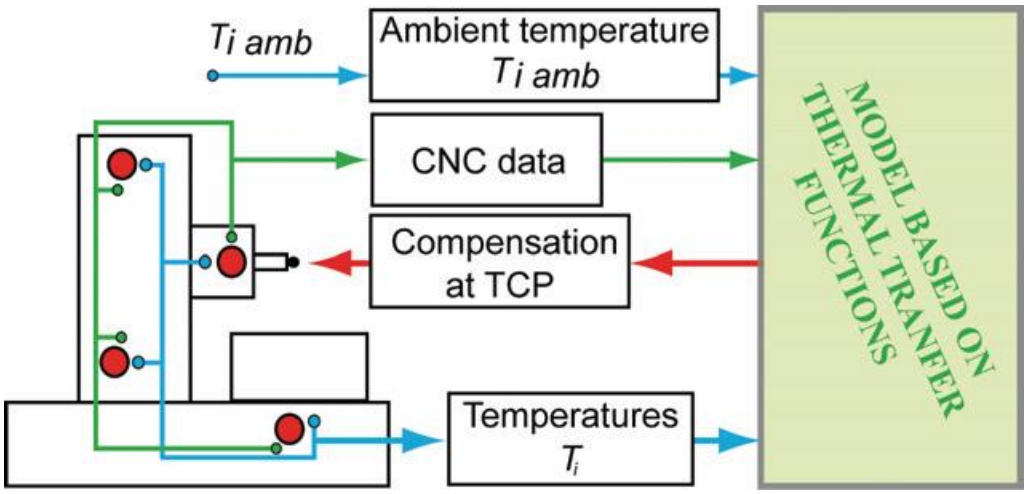

Fig. 8 Scheme of the indirect compensation method based on thermal transfer function model [28].

Some of the used methods of thermal software compensation are listed and described in the following sections.

3.4.1 Multiple linear regression analysis (MLRA)

Regression analysis uses polynomials to compensate for thermal deformations of MT. Polynomials coefficients can be obtained from calibration measurements. This method solves the relationship between quantitative variable responses and one or more quantitative explanatory variables. The analysis is relatively simple and can be easily applied in most modern control systems and. The disadvantage of this method is the necessity of a higher number of input variables (tending to collinearity) to reach intended accuracy, so results are not easily transferable to other MTs. The accuracy depends on the number of temperature sensors, their location, the method of calibration of coefficients, and the number of calibration measurements [25].

One of the most used methods of software compensation of thermal errors of MT is **Multiple linear regression analysis (MLRA)** [29]. The MLRA is used when there is more than one variable (e.g., temperatures of different points on the spindle unit, spindle speed, etc.). Equation (2) describes the most used regression model of a multilayer temperature error model.

$$\delta = Y \cdot \beta \quad (2)$$

Correction coefficient β can be calculated using the equation (3):

$$\beta = (Y^T \cdot Y)^{-1} \cdot Y^T \cdot \delta \quad (3)$$

The method can be improved by advanced estimation of correction coefficients [30] and mechanisms defining key temperature points to minimise the variable input amount and avoid collinearity [31].

3.4.2 Finite element method (FEM)

The finite element method (FEM) or the finite difference method (FDM), or a combination of both methods, can be used to model the temperature conditions of MT. The wider use of some of these methods for real-time compensation is not yet possible due to the long computational time. A partial solution to the issue is the use of MOR (model order reduction) with the help of Krylov subspace method. The use of MOR reduce computing time significantly, and models are suitable even for real-time applications. The main obstacle to wider application in real-time compensation is the MOR application capability only within one MT configuration [32]. However, FEM is very useful in the design phase of MT construction. The complexity of the calculation is given mainly by a large number of parameters, boundaries, and initial conditions (see Fig. 9). In addition, these parameters cannot often be determined exactly [33].

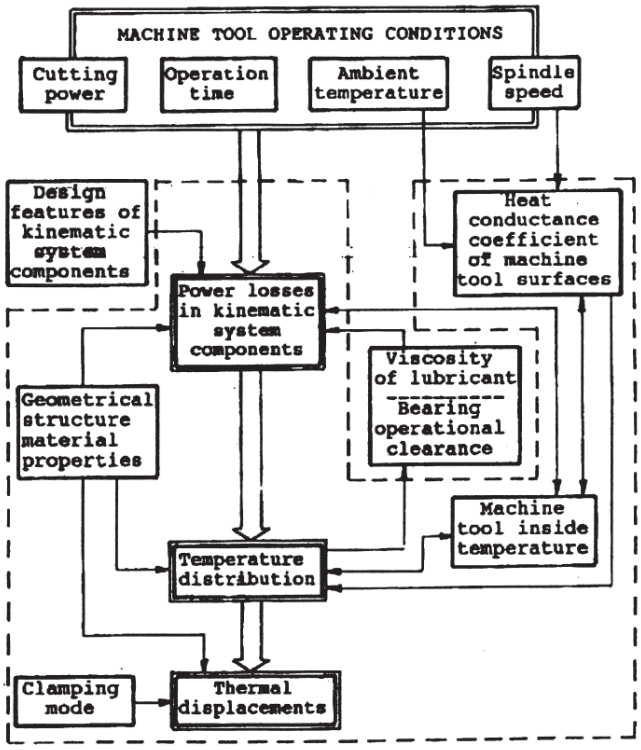

Fig. 9 Links between factors affecting the thermal state of a MT [14].

3.4.3 Artificial neural network (ANN)

A neural network is essentially an instrument of computer data processing. It is a "package" of particular points (neurons) interconnected and pass information to each other by using transfer functions. The target of ANN is to determine outputs based on a large number of simple input operations. The considerable advantage of a neural network is the ability to work with broken or incomplete input data. When using ANN, it is essential to choose the appropriate learning mode, in which the system learns (from temperature sensors data) to predict output vectors approximating the temperature behaviour of the MT [29]. However, models based on neural networks have a closed structure (also called "black box"), which makes it impossible to transfer them between different MTs (including MTs of the same type and size), and the model cannot be simply extended by other heat sources than those

with which it was calibrated. ANN and derived methods are suitable for MT learning principles with a certain potential in intelligent MT concepts.

3.4.4 Transfer functions

Transfer functions (*TF*) can describe the relationship between input (excitation *E*) and output (response *R*) parameters of a dynamic system (equation (4)).

$$TF(s) = \frac{R(s)}{E(s)} \quad (4)$$

Transfer functions can be compiled in several ways [34]:

- **Analytically and following calibration of the system** – use only for geometrically simple tasks; transfer function constants are determined during calibration.
- **Estimation and following calibration of the system** – an estimate of the function from the response measured during unit step function excitation; the transfer function constants are determined during calibration.
- **Estimation with following optimization of the system** – estimation of the function from the response measured during general excitation; transfer function constants are determined during optimization.

The undeniable advantage of the transfer function is that they can solve individual heat sources separately (drives, gears, spindle rotation, machining process). From these mutually independent functions, it is then possible to compile one complex model for compensation of thermal deformations of the MT [34].

In [35], Uriarte performs a complete analysis of the mathematical apparatus called Thermal Modal Analysis, an analogy to the commonly known Modal Analysis of oscillating properties of mechanical systems. The analogy between dynamic and temperature analysis is expressed in Fig. 10.

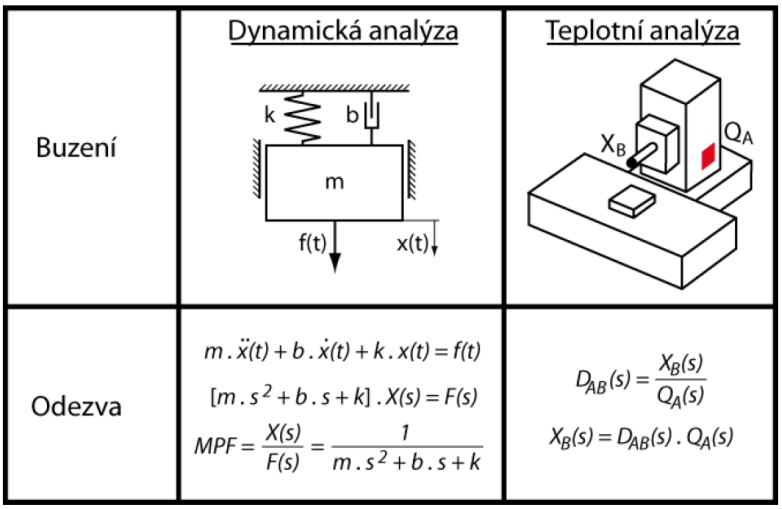

Fig. 10 Comparison between temperature and dynamic analysis [2].

In [27], transfer functions are used in an adaptive self-learning model application (so-called hybrid model; a combination of direct and indirect compensation methods) to estimate thermal errors during the long term and various MT activity processes with activity within untrained inputs to the thermo-mechanical system.

3.5 Methods of calibration tests for obtaining input data for software compensation models of thermal errors of MT

Calibration measurements are required to obtain input data to the thermal compensation model. Some of the ways to perform calibration measurements are listed below.

Basic calibration tests are described in the ISO standard. The ISO 230-3 standard [36] was created to determine the thermal influences acting on the MT. It consists of four types of tests:

- an environmental temperature variation error (ETVE) test,
- a test for thermal distortion caused by rotating spindles,
- a test for thermal distortion caused by moving linear axes,

- a test for thermal distortion caused by the rotary motion of components.

The standard specifies the conditions under which tests should be performed. The MT must be functional and fully assembled during the test. It must be set up on the base and supplied with energy during the test. The MT and the measuring device must be protected against drafts and other external temperature influences. All tests are performed under no-load MT operating and using all MT compensation systems. The test is performed at a MT ambient temperature of 20 °C, or a nominal differential thermal expansion (NDE) correction is used [10].

Due to the measurement conditions, it is clear that the test does not include the temperature effect of the cutting process of the MT [10].

In this work, a test of thermal deformations caused by spindle rotation (also known as aircut) is selected to measure calibration tests. The measurement is performed using non-contact sensors (inductive, capacitive, or eddy current sensors), placed in a stand clamped to the MT table, and measured the position of the rotating mandrel clamped in the MT spindle (Fig. 11).

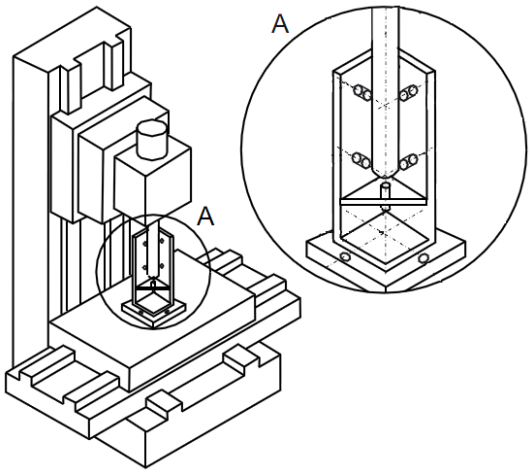

Fig. 11 Test of thermal errors caused by spindle rotation according to the standard ISO 230-3 [10].

The disadvantage of the calibration measurement performed by the aircut test is that it does not correspond to the real load operating MT (during machining of the workpiece) and that it is performed only at one point of the working space of the

MT. For this reason, studies of new methods of performing calibration tests eliminating the disadvantages mentioned above are the subject of current research. This is, for example, a stressing unit connected to the spindle [37] or increasing the current load of the spindle by its repeated turning and braking [28]. However, the conclusions from [38] show that if the deformation measurement at TCP is not performed with the inclusion of a real cutting process, the results generated by the thermal compensation model are not acceptable. Some calibration tests, including the influence of a real cutting process, are performed in [39, 40] - the real issue is to gather reliable information from a measurement of MT deformation at TCP during the continuous machining process. Another approach is to machine and subsequent measurement of a test workpiece [41].

4 Influence of input parameters of thermal error model

Nowadays, thermal errors are the main source of machining errors (as the above research shows). One way to reduce them is to use a compensation model. Inputs to the compensation model are usually temperatures measured at significant heat sources (see section 3.4). Results from previous years [42–44] suggest that some temperature inputs might correlate with the thermal behaviour of the MT structure better than the others. In this section, compensation models with 3 different temperature sources as inputs will be set up and compared with each other.

4.1 Experimental set-up

4.1.1 Target machine

Measurements were performed on a 5-axis milling center of the upper gantry type. The maximum workpiece size that can be clamped to the rotary table is 700 mm. The MT is placed in the RCMT laboratory. It is an unconditioned room with a relatively low ceiling, and the MT is located near an external door (often used for ventilation). In total, in terms of temperature stability, it is not an entirely suitable space. Other technological equipment of the laboratory is also located near the MT.

A schema of the basic structure of the target machine with the approximate location of the measuring sensors (detailed further in section 4.1.2) is shown in Fig. 12.

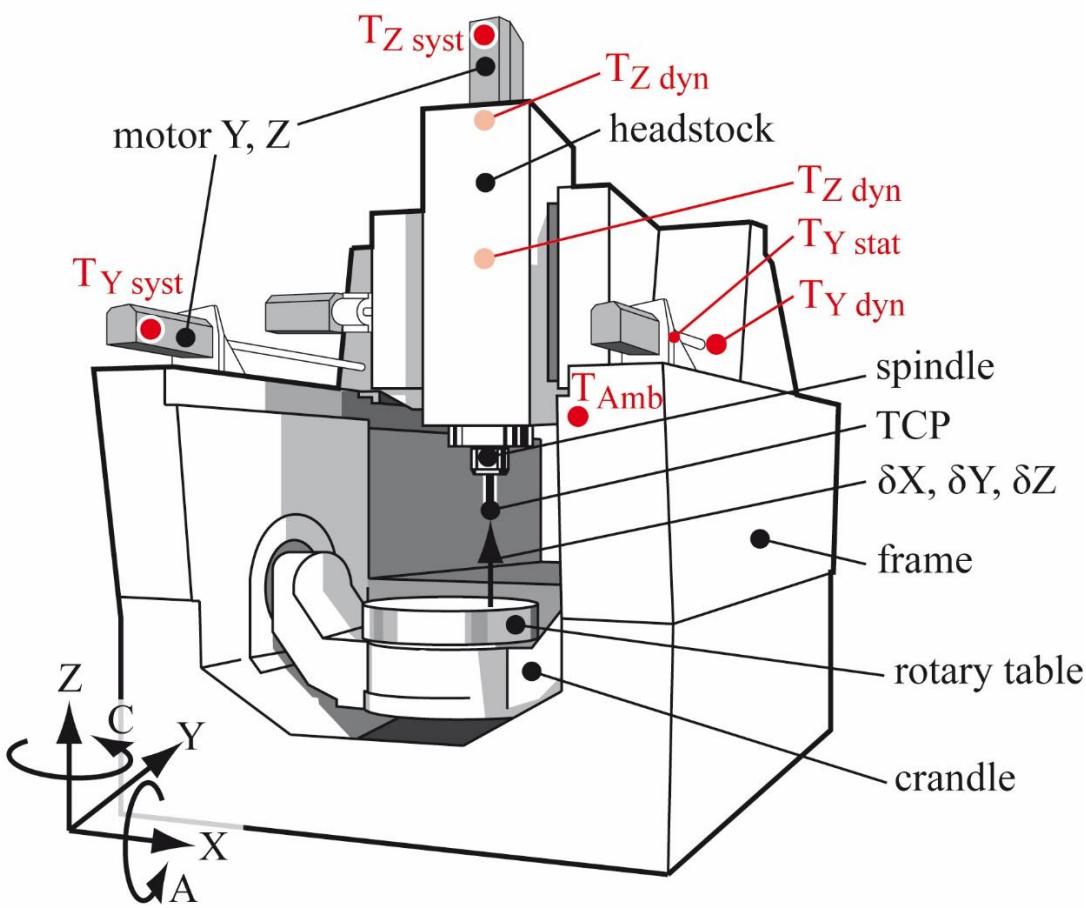

Fig. 12 Schema of the target machine structure with approximate positions of temperature and deformation sensors [42].

4.1.2 Measurement

The use of other temperature inputs could lead to an improvement in the approximation quality of the model compensating for thermal errors caused by motion in the linear axes of the MT [42–44]. Originally, only the temperature input from a motion linear axis motor (introduced into the MT control system for diagnostic purposes) was used (the temperatures are recorded in 1 K resolution). The measured MT was equipped with additional temperature sensors (Pt100, Class A, 3850 ppm/K) placed on a bearing house of the ball screw bearing (see Fig. 13). The bearing house is a static element; the installation of the sensor is relatively easy.

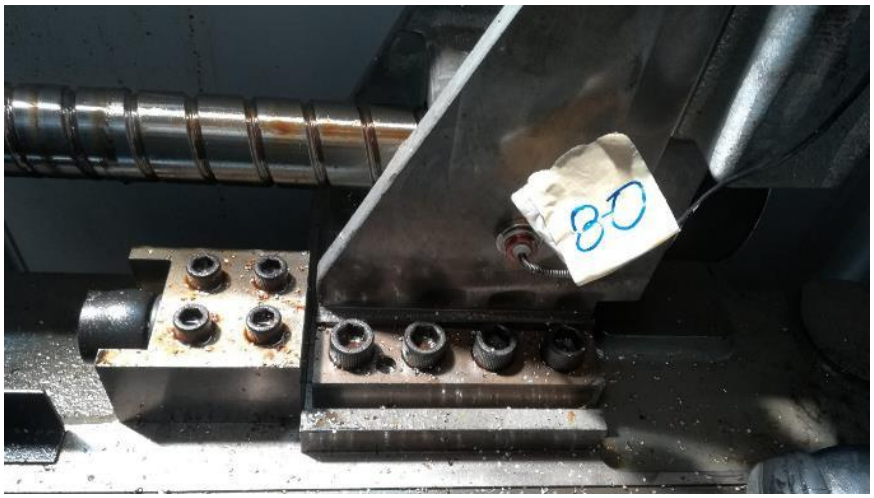

Fig. 13 External temperature sensor placed on the static element (bearing house of the ball screw bearing).

The MT was further equipped with additional sensors to measure the temperature at the front side of a ball screw nuts (see Fig. 14). The ball screw nut is a moving element; the installation of the sensor is complicated. There is an expectation that this temperature could have the best correlation with the thermal behaviour of the MT structure when moving in linear axes [43].

Fig. 14 External temperature sensor placed on the dynamic element (front side of the ball screw nut).

Several additional temperature sensors were also placed on the MT; however, only the sensor located at the top of the MT frame was used within the thesis. The temperature proved to be the most suitable for interpretation of the ambient temperature changes.

All measurements were performed in accordance with the ISO 230-3 standard (see section 3.5) without loading the MT with the cutting process. A test mandrel (representing a TCP) was clamped in the spindle holder for measurement purposes. The deformation at the TCP was measured in 3 linear directions (X, Y, Z – see Fig. 15; no angular deformations are considered) using non-contact eddy-current sensors PR6423 (Emerson). All measured data during the experiments were acquisitioned in CompactRio-9012 diagnostic control panel by National Instruments.

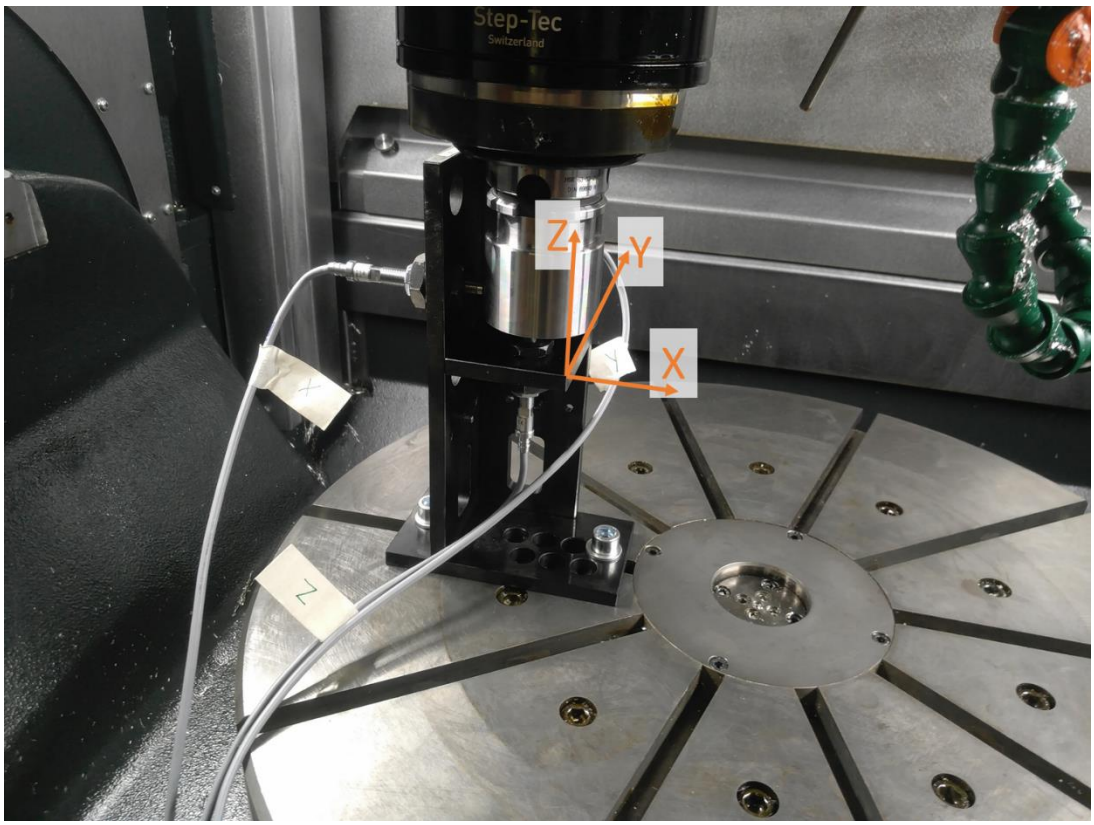

Fig. 15 The position of the deformation measuring sensors at the TCP with the displayed MT coordinate system.

Table 1 lists all measured variables with a short description of the location of sensors (also in Fig. 12) measuring the temperatures and deformations exploited within the thesis.

Table 1 All measured variables with a short description of the location of sensors.

Measured variables			
temperature [K]		deformation [μm]	
$T_{Y\ syst}$	sensor in motor of linear axis Y	δX	deformation at TCP in X direction
$T_{Z\ syst}$	sensor in motor of linear axis Z	δY	deformation at TCP in Y direction
$T_{Y\ stat}$	sensor on bearing house of the bearing screw in the Y direction	δZ	deformation at TCP in Z direction
$T_{Z\ stat}$	sensor on bearing house of the bearing screw in the Z direction	-	-
$T_{Y\ dyn}$	sensor on front side of the ball screw nut in the Y direction	-	-
$T_{Z\ dyn}$	sensor on front side of the ball screw nut in the Z direction	-	-
T_{amb}	ambient temperature	-	-

Table 2 shows all performed measurements. The tests were performed at different constant feed rates in the directions of the linear motion axes Y, Z. The movement in the linear X-axis is behind the scope of this thesis.

Table 2 Performed experiments.

No.	Inspected thermal error	Heat source	Feed rate [$m \cdot min^{-1}$]
1a	XTY, YTY, ZTY	Y feed drive	10
1b	XTZ, YTY, ZTZ	Y feed drive	5
1c	XTY, YTY, ZTY	Y feed drive	15
2a	XTZ, YTY, ZTZ	Z feed drive	10
2b	XTY, YTY, ZTY	Z feed drive	5
2c	XTZ, YTY, ZTZ	Z feed drive	15

It is not possible to move linearly in a specific direction at a constant feed rate for a sufficiently long time due to the finite dimensions of the MT. Therefore, the measurements were performed by moving the TCP out of the base position (the point at which the TCP deformations are measured) and began to move at a constant feed rate in a specific direction. After reaching the end position of the MT's workspace,

the direction of motion reversed, and the TCP began to move at a given constant feed rate in a specific linear direction to the other end position of the workspace. This activity (loading phase) continued for 20 minutes. The TCP returned to the base position then, where the TCP deformations measurement was performed for 10 seconds (measuring phase). This whole process (cyclical repetition of loading and measuring phases) was performed for 8 hours. This period is called the heating phase. After the heating process, the TCP returned to the base position, and then the measurement of deformations was performed for 16 hours – it's called the cooling phase. The experiment was considered finish after both the heating and the cooling phase were executed.

Not every measurement contains the cooling phase due to the failure of the diagnostic control panel.

4.1.3 Normalization of measured data

After the measurements were made, the measured data had to be processed and interpreted correctly. This is important for deformations at TCP, not in the case of temperatures. In this work, the measured data were interpreted in accordance with the MT coordinate system (see Fig. 12). For example, when TCP moves 1 µm relative to the initial position (closer to the table) in the MT Z-axis, the change must be reflected as a "minus" 1 µm in the measured deformation vector in the same direction.

All measured deformational data were unified in this way. Due to the sensor's principle (the closer the measured object is to the sensor, the smaller the voltage value is recorded) was necessary to multiply the vector of measured deformations in the Y direction by "minus" 1 to align it directionally with the MT coordinate system. The location of the deformation measuring sensors at the TCP with the MT coordinate system was shown in Fig. 15.

Eddy-current sensors have to be calibrated before measurements start because the raw measured outputs are voltage. This was performed by the so-called "jump" test in the individual linear axes of the MT. For example, the measurement for the Z-axis was performed by starting the deformation measurement at the diagnostic station. At that moment, the measuring mandrel was in the basic position. Then the TCP was moved by 100 µm in the positive direction of the linear Z-axis (using a command in the MT control system), and then the measurement was performed for 10 seconds. Then the TCP was moved by 100 µm in the negative direction of the same axis, and the measurement was performed. Measured data were subsequently analysed (based on the knowledge of the position change from the control system) to determine the conversion coefficients from the measured voltage change to the deformation change in µm. The measured voltage curves from the "jump" tests are shown in Fig. 16.

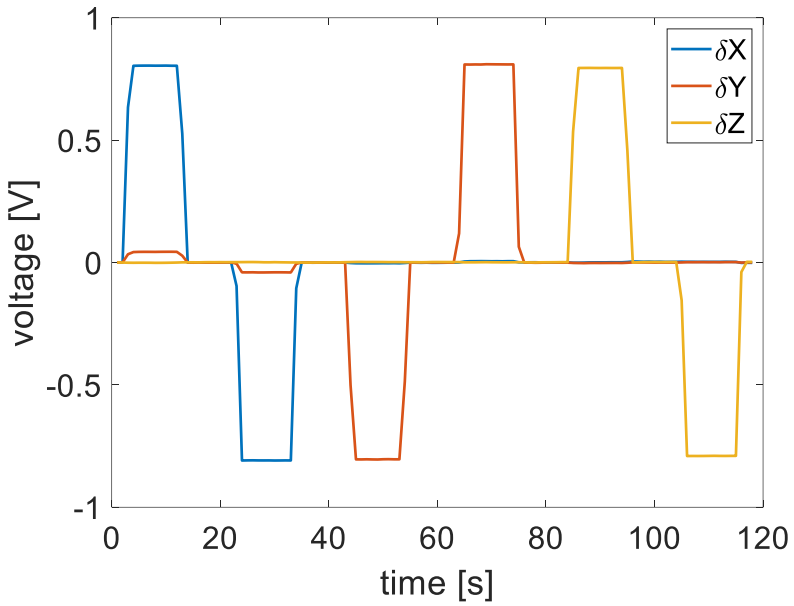

Fig. 16 Measured voltage during "jump" tests.

4.2 Evaluation of approximation quality

The approximation quality of the simulated behaviour is expressed by equation (5). This value represents the percentage of the output deviation

generated by the model [45]. The evaluation is based on the least squares approximation method. The value 100 % expresses the complete agreement of the measured and simulated behaviour; the time progress of deformation in this case. The *FIT* value is called a "global" indicator of the approximation quality.

$$FIT = \left(1 - \frac{\|\delta Z - \delta Z_{SIM}\|}{\|\delta Z - \overline{\delta Z}\|}\right) \cdot 100. \quad (5)$$

The vector norm used in equation (5) is expressed by equation (6), where δ is a general vector of length *r* [45].

$$\|\delta\| = \sqrt{\delta_1^2 + \delta_2^2 + \cdots + \delta_r^2} \quad (6)$$

The approximation error is also expressed by a residue value (equation (7)) representing a fictive thermal deformation obtained after implementation and activation of the compensation algorithm in the MT control system [46]. It is simply the difference between measured and simulated deformations. The *RES* value is a "local" indicator of the approximation quality.

$$RES = \delta Z - \delta Z_{SIM} \quad (7)$$

There is a difference between these two methods. The *FIT* method evaluates the approximation quality by just one number in percent, while the *RES* gives information about approximation quality at every single point of measured and simulated deformations. It can also be applied peak-to-peak method (equation (8)) for global evaluation (after using the residuum method), giving information about the worst absolute approximation quality from the whole measured or *RES* vector.

$$PTP = |\delta Z_{max}| + |\delta Z_{min}|. \quad (8)$$

All calculations and graphical outputs were performed in MATLAB (version R2020a).

4.3 Calibration of compensation model

The development of the software indirect thermal compensation model starts by performing several measurements. One measurement (called calibration) is used to create the compensation model. In general, the compensation model describes the link between the input (the temperature change at the heat source in this thesis) and the output (the deformation at the TCP). Therefore, the calibration measurement is used to "train" the model behaviour in a given dynamic system (a MT in this case). Generally, calibration should describe a transient characteristic between two thermodynamic equilibria; one with the MT surroundings and one with all active thermal sinks and sources meant to be approximated.

Further is necessary to check whether the "training" was done correctly. In other words, if the thermal behaviour of the specific dynamical system is described correctly and linearly. For this reason, another measurement (called verification) is performed when one of the relevant parameters is changing. Here, the change in the feed rate (to check the model's efficiency and define limit parameters to obtain sufficient approximation quality) is taken into account.

Several types of compensation models were described in section 3.4. A compensation model based on the transfer functions principle was selected to predict and compensate for thermal errors (see section 3.4.4) within the thesis.

Two of the most common linear parametric models were used; the *Autoregressive model with external input* (ARX) and the *Output error model* (OE) [47]. These methods allow establishing the model parameters from sequences of measured input *u* and output *y* values.

The resulting transfer identified by one of the methods (ARX, OE) is described in general form by equation (9).

$$y(t) = \varepsilon \cdot u(t) \qquad (9)$$

The transfer function in a time-discrete region, where a_n is the calibration coefficient of the transfer function input and b_m is the calibration coefficient of the transfer function output (obtained by estimating the transfer function using the ARX or OE method), is expressed by the following equation (10):

$$y(k) = \frac{u(k-n)\cdot a_n + \cdots + u(k-1)\cdot a_1 + u(k)\cdot a_0}{b_0} - \left(\frac{y(k-m)\cdot b_m + \cdots + y(k-1)\cdot b_1}{b_0}\right), \qquad (10)$$

where *k* describes a given time instant, the parameters *n* and *m* are orders of the transfer functions numerator (*n*) and denominator (*m*), and *k*-*n* (or *k*-*m*) is the delay in sampling frequency. The equation (10) expresses the wanted output *y(k)* and is written in differential form.

The identification of the transfer functions was performed on calibration measurements at a constant feed rate of 10 m·min^{-1} (1a and 2a in Table 2) in linear axes Y, Z. The deformations in the X, Y, and Z directions were measured at TCP. The calibration was done only within the heating phase. A possible simplification and time-saving are the main reasons. Furthermore, it was not possible to measure the cooling phases within all measurements. Future research work (over the scope of this thesis) deals with this phenomenon in proper detail.

Three temperature inputs to the compensation model were available (T_{syst}, T_{stat}, T_{dyn}; see Table 1) for the activity of each thermal source (movement in a linear axis). Compensation models per each combination of inputs and outputs were built up. Calculations of simulated deformations for specific directions, temperature inputs, and tests are given in equations (11) to (15), where *in* = syst (T_{syst}), stat (T_{stat}), dyn (T_{dyn}).

$$XTY_{in} = \Delta T_{in} \cdot \varepsilon_{in}^{XTY} \qquad (11)$$

$$XTZ_{in} = \Delta T_{in} \cdot \varepsilon_{in}^{XTZ} \qquad (12)$$

$$YTY_{in} = \Delta T_{in} \cdot \varepsilon_{in}^{YTY} \qquad (13)$$

$$ZTY_{in} = \Delta T_{in} \cdot \varepsilon_{in}^{ZTY} \qquad (14)$$

$$ZTY_{in} = (\Delta T_{in} - \Delta T_{amb}) \cdot \varepsilon_{in}^{ZTY} + \underbrace{\Delta T_{amb} \cdot \varepsilon_{amb}}_{Z_{amb}} \quad (15)$$

$$ZTZ_{in} = (\Delta T_{in} - \Delta T_{amb}) \cdot \varepsilon_{in}^{ZTZ} + \underbrace{\Delta T_{amb} \cdot \varepsilon_{amb}}_{Z_{amb}} \quad (16)$$

Models were extended to description of thermal error at TCP caused by ambient temperature changes. For this purpose, a measurement with no active internal thermal source over 26 hours was performed. The thermal compensation model (Z_{amb}) concerning the influence of the ambient temperature in the Z direction was set up. The influence of the ambient temperature on the thermal error in the X and Y directions at TCP is minor and not include in compensation efforts.

Using the transfer function with a maximum order of 4 (the maximum value of the parameters *m, n*) is a recommendation of the thesis supervisor. All ARX and OE functions were generated (with the help of Matlab Identification Toolbox [48]) for a mutual combination of *m* and *n* parameter values from 1 to 4. The function with the best-obtained approximation quality value (*FIT* in this case) compared to the others is selected into the modelling process. Coefficients (a_n, b_n) of the identified transfer functions describing Y and Z axis movement influence on a thermal error in the X, Y, and Z directions of MT are stated in Annex 1.

Behaviours of measured temperatures (models XTY_{in},…,ZTZ_{in} inputs), feed rates, measured and simulated deformations (outputs) in the directions of the MT coordinate system (X, Y, Z) for tests No. 1a and 2a are shown in Fig. 17 to Fig. 22. Interrelated input-output pairs are drawn in the same colour (ΔT_{syst} and XTY_{syst}, XTZ_{syst}, YTY_{syst}, YTZ_{syst}, ZTY_{syst}, ZTZ_{syst} in red; ΔT_{stat} and XTY_{stat}, XTZ_{stat}, YTY_{stat}, YTZ_{stat}, ZTY_{stat}, ZTZ_{stat} in green; ΔT_{dyn} and XTY_{dyn}, XTZ_{dyn}, YTY_{dyn}, YTZ_{dyn}, ZTY_{dyn}, ZTZ_{dyn} in purple). The ambient temperature (ΔT_{amb}) is drawn in brown and measured (in short mea) deformations XTY_{mea}, XTZ_{mea}, YTY_{mea}, YTZ_{mea}, ZTY_{mea}, ZTZ_{mea} in black. Note that ZTY_{mea} and ZTZ_{mea} deformations are already compensated from the influence of the ambient environment by the Z_{amb} model.

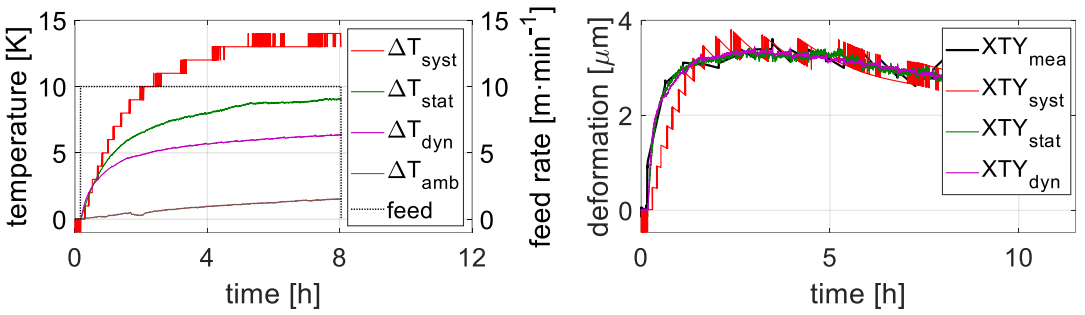

Fig. 17 Behaviours of measured temperatures and Y-axis feed rate (left) and behaviours of measured and simulated deformations in the X direction (right) during test No. 1a.

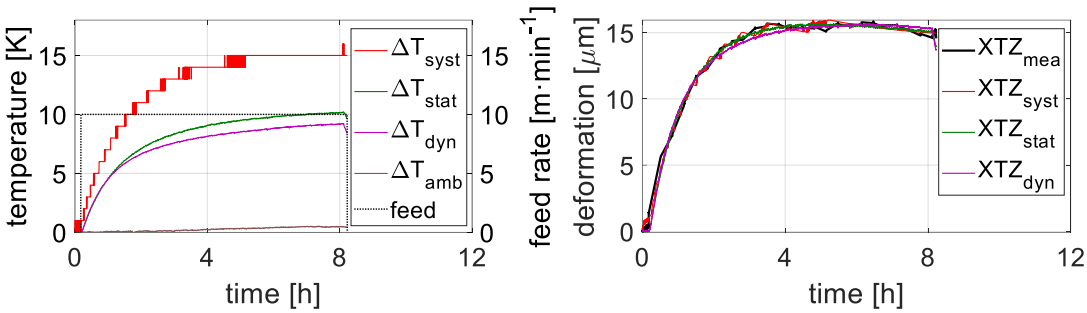

Fig. 18 Behaviours of measured temperatures and Z-axis feed rate (left) and behaviours of measured and simulated deformations in the X direction (right) during test No. 2a.

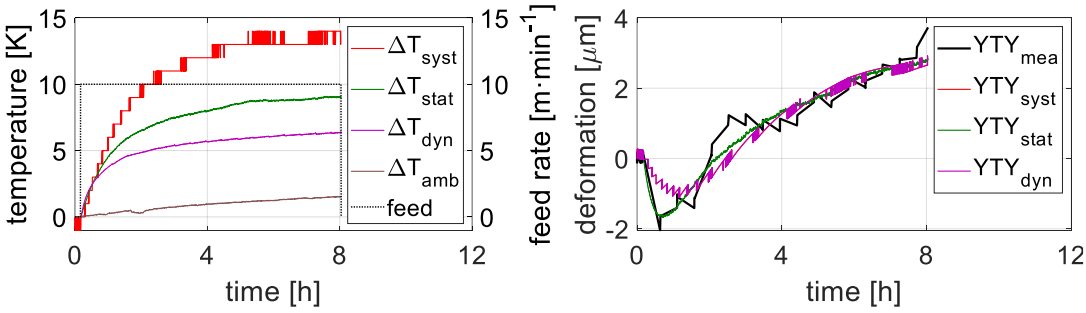

Fig. 19 Behaviours of measured temperatures and Y-axis feed rate (left) and behaviours of measured and simulated deformations in the Y direction (right) during test No. 1a.

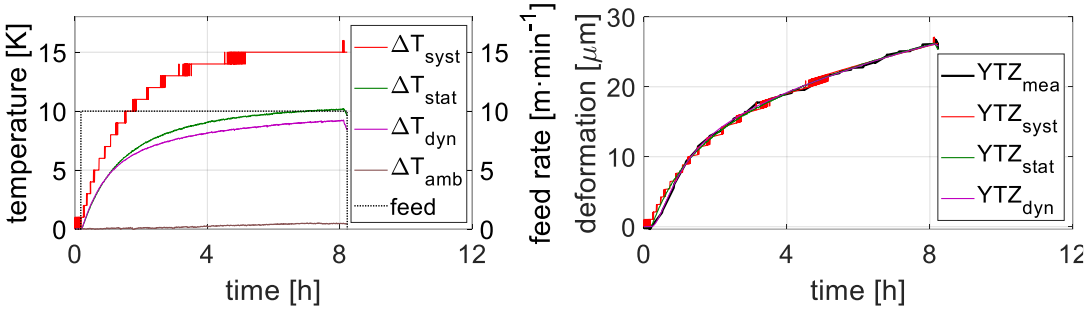

Fig. 20 Behaviours of measured temperatures and Z-axis feed rate (left) and behaviours of measured and simulated deformations in the Y direction (right) during test No. 2a.

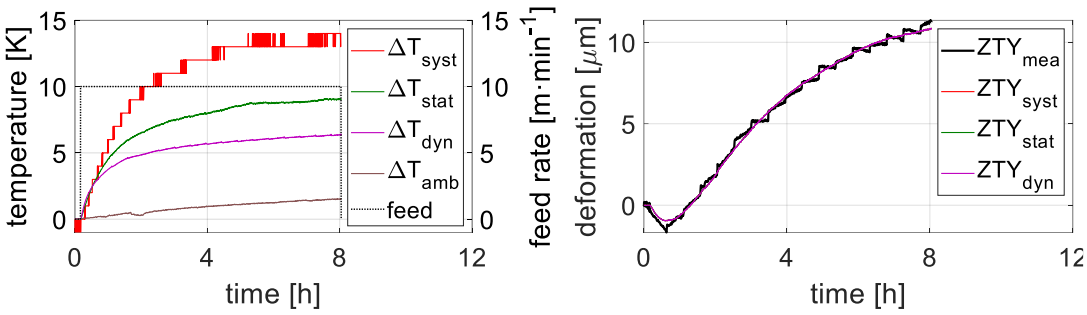

Fig. 21 Behaviours of measured temperatures and Y-axis feed rate (left) and behaviours of measured and simulated deformations in the Z direction (right) during test No. 1a.

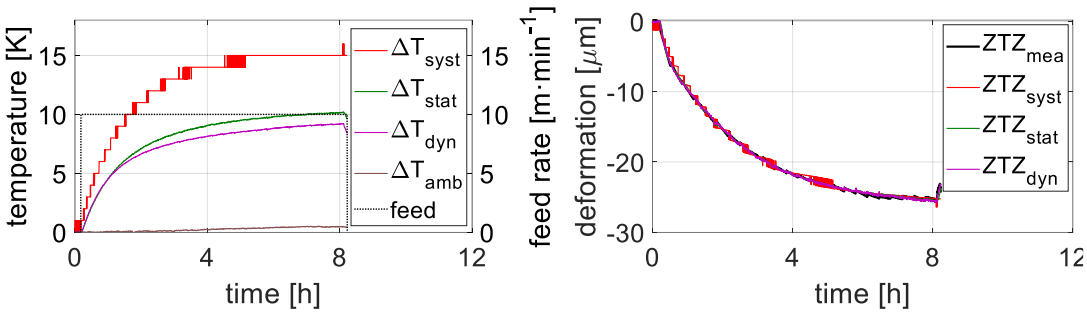

Fig. 22 Behaviours of measured temperatures and Z-axis feed rate (left) and behaviours of measured and simulated deformations in the Z direction (right) during test No. 2a.

The following 3 contains information regarding the type and the order of transfer functions selected to compensate thermal error along with model input temperature and FIT approximation quality value. Note that only the heating phases are evaluated.

Table 3 Basic parameters of the developed compensation models with FIT and response test results.

Model of thermal error	T_{in}	Type	Order (m,n)	*FIT* [%]
XTY	T_{syst}	ARX	1,2	29
	T_{stat}	OE	3,3	73
	T_{dyn}	OE	4,4	74
XTZ	T_{syst}	OE	3,2	91
	T_{stat}	OE	2,1	89
	T_{dyn}	OE	2,2	88
YTY	T_{syst}	ARX	1,2	65
	T_{stat}	OE	3,2	76
	T_{dyn}	ARX	1,2	72
YTZ	T_{syst}	OE	3,1	92
	T_{stat}	OE	2,1	94
	T_{dyn}	ARX	2,2	97
ZTY	T_{syst}	ARX	1,2	92
	T_{stat}	ARX	1,2	95
	T_{dyn}	ARX	1,2	95
ZTZ	T_{syst}	ARX	1,2	93
	T_{stat}	OE	3,4	96
	T_{dyn}	OE	4,2	97
Z_{amb}	T_{amb}	ARX	1,4	59

Checking the stability of the model is also essential during the selection of the appropriate transfer function setting. LTI step response test [48], where the input variable (in this case, the temperature) is a unit change, was used. The resulting behaviour of the output variable in the step response test should not be oscillated and should return to the original value (zero in this case). The LTI tests charts for each identified transfer function are shown in Annex 1.

It can be seen that there is no significant difference between the inputs of the calibrated functions.

4.4 Verification of compensation model

Verification is an important and necessary part of developing a thermal compensation model. It is used to examine as many possible states that can occur during the operation of the described source or heat sink [2]. The verification tests

are used to examine the linear behaviour of described (active) thermal sources. For these purposes, measurements were performed during the MT linear motion axis activity at feed rates of 5 and 15 m·min^{-1} - tests 1b, 1c, 2b, and 2c (see Table 2).

Models developed in section 4.3 are applied on verification measurements in the following sections 4.4.1 and 4.4.2.

4.4.1 Test 1b and 2b

Behaviours of measured temperatures (models XTY_{in},…,ZTZ_{in} inputs), feed rates, measured and simulated deformations (outputs) in the directions of the MT coordinate system (X, Y, Z) for tests No. 1b and 2b are shown in Fig. 23 to Fig. 28. Note that ZTY_{mea} and ZTZ_{mea} deformations are already compensated from the influence of the ambient environment by the Z_{amb} model.

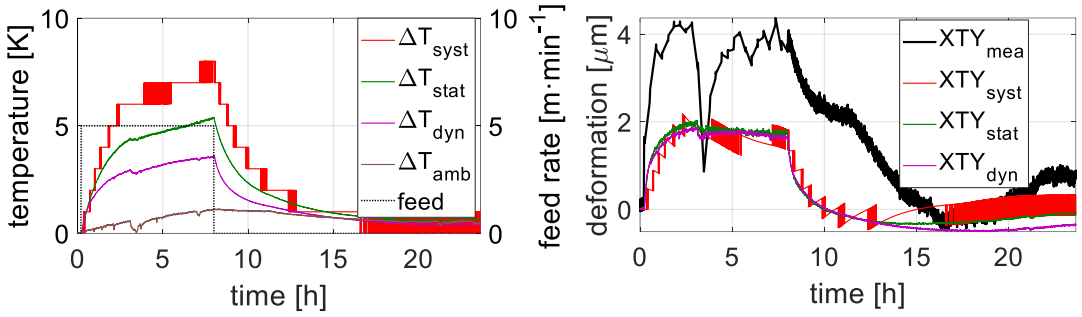

Fig. 23 Behaviours of measured temperatures and Y-axis feed rate (left) and behaviours of measured and simulated deformations in the X direction (right) during test No. 1b.

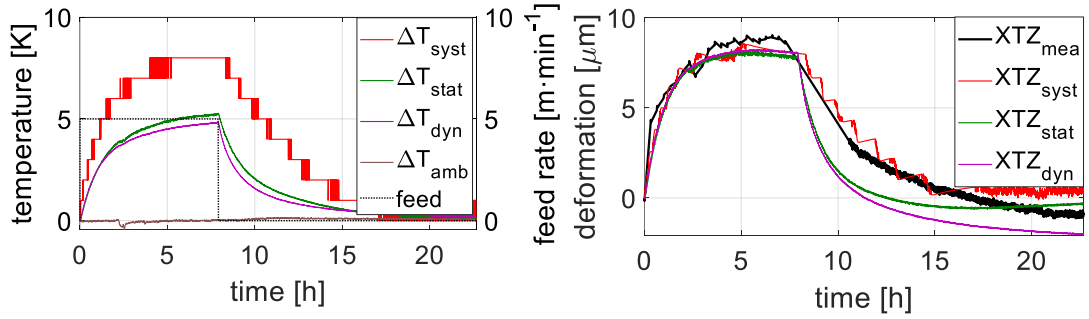

Fig. 24 Behaviours of measured temperatures and Z-axis feed rate (left) and behaviours of measured and simulated deformations in the X direction (right) during test No. 2b.

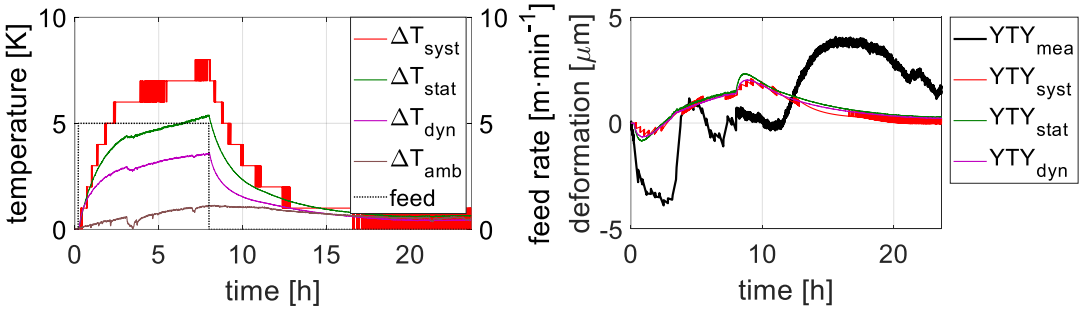

Fig. 25 Behaviours of measured temperatures and Y-axis feed rate (left) and behaviours of measured and simulated deformations in the Y direction (right) during test No. 1b.

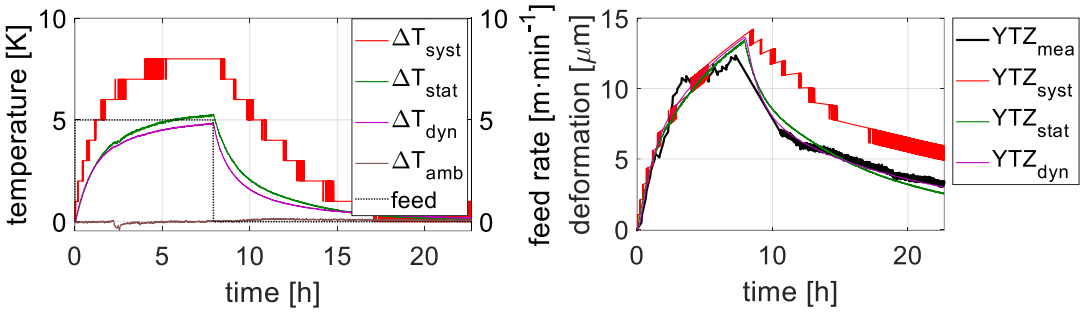

Fig. 26 Behaviours of measured temperatures and Z-axis feed rate (left) and behaviours of measured and simulated deformations in the Y direction (right) during test No. 2b.

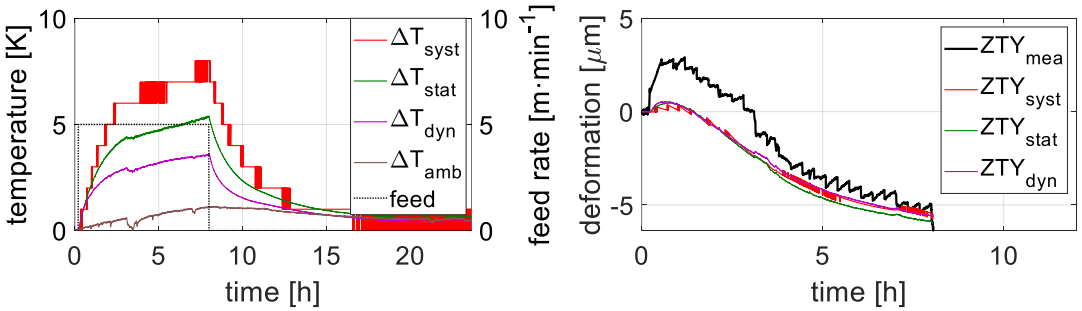

Fig. 27 Behaviours of measured temperatures and Y-axis feed rate (left) and behaviours of measured and simulated deformations in the Z direction (right) during test No. 1b.

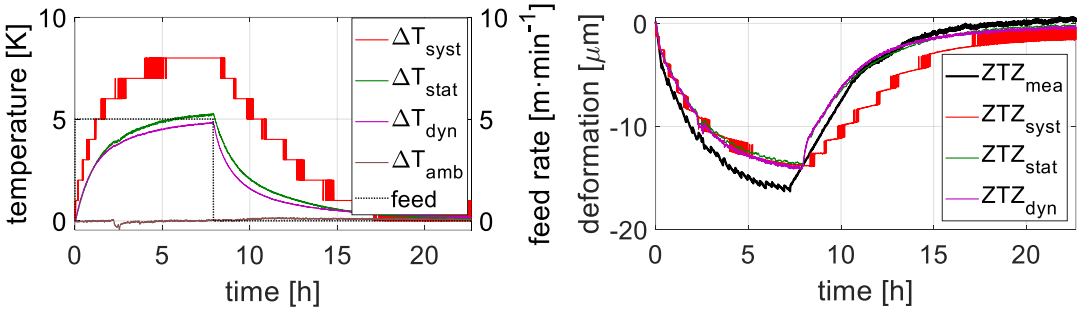

Fig. 28 Behaviours of measured temperatures and Z-axis feed rate (left) and behaviours of measured and simulated deformations in the Z direction (right) during test No. 2b.

4.4.2 Test 1c and 2c

Behaviours of measured temperatures (models XTY_{in},…,ZTZ_{in} inputs), feed rates, measured and simulated deformations (outputs) in the directions of the MT coordinate system (X, Y, Z) for tests No. 1c and 2c are shown in Fig. 29 to Fig. 34. Note that ZTY_{mea} and ZTZ_{mea} deformations are already compensated from the influence of the ambient environment by the Z_{amb} model.

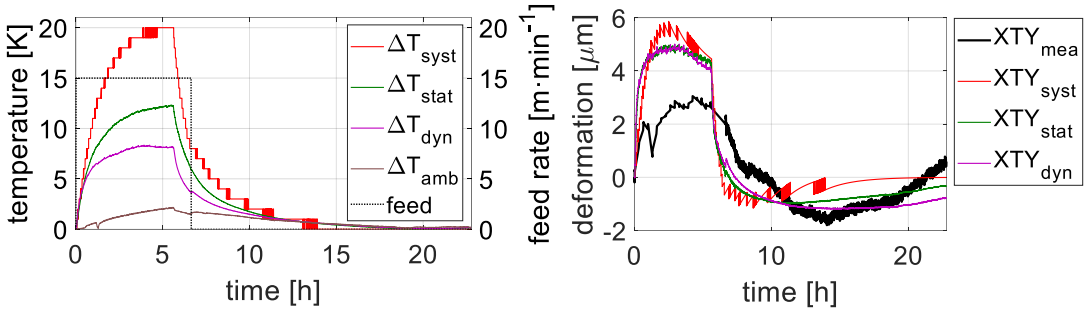

Fig. 29 Behaviours of measured temperatures and Y-axis feed rate (left) and behaviours of measured and simulated deformations in the X direction (right) during test No. 1c.

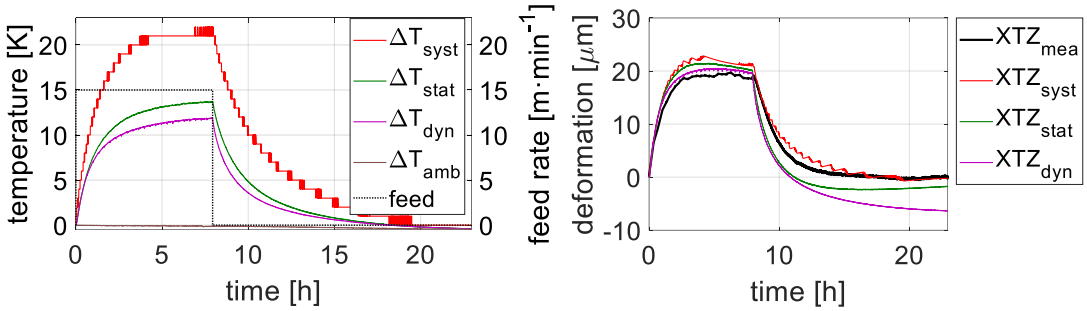

Fig. 30 Behaviours of measured temperatures and Z-axis feed rate (left) and behaviours of measured and simulated deformations in the X direction (right) during test No. 2c.

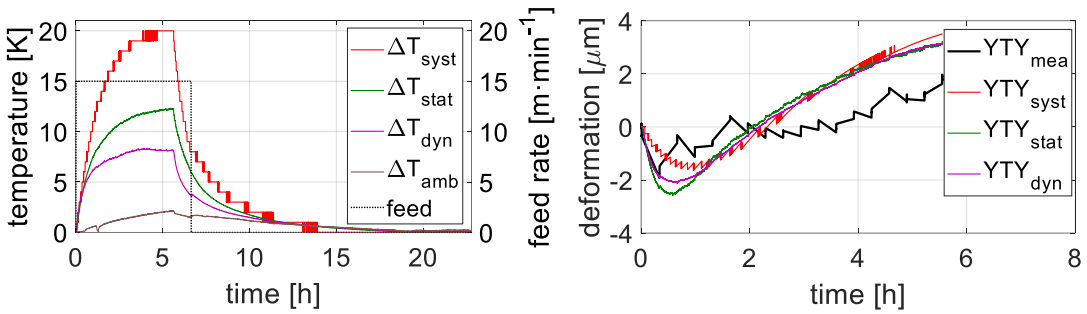

Fig. 31 Behaviours of measured temperatures and Y-axis feed rate (left) and behaviours of measured and simulated deformations in the Y direction (right) during test No. 1c.

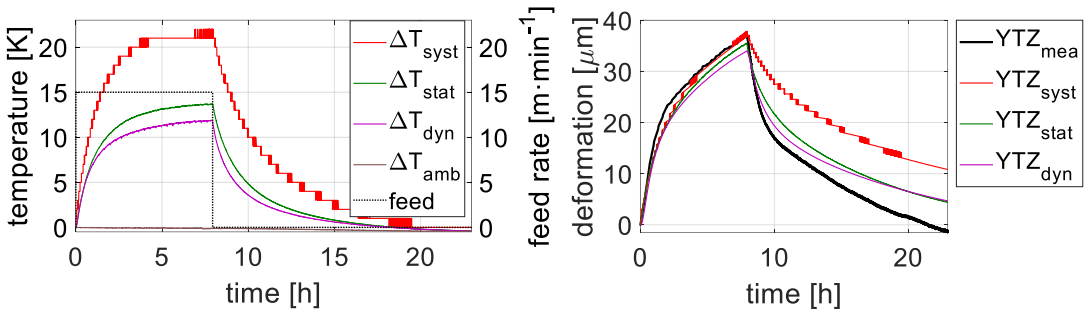

Fig. 32 Behaviours of measured temperatures and Z-axis feed rate (left) and behaviours of measured and simulated deformations in the Y direction (right) during test No. 2c.

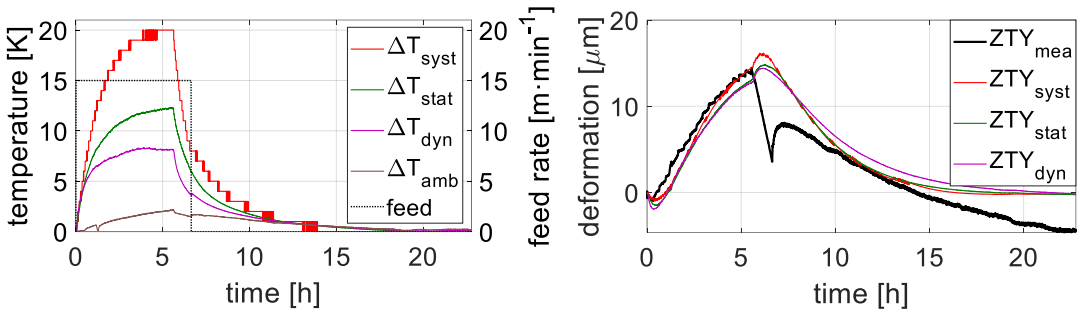

Fig. 33 Behaviours of measured temperatures and Y-axis feed rate (left) and behaviours of measured and simulated deformations in the Z direction (right) during test No. 1c.

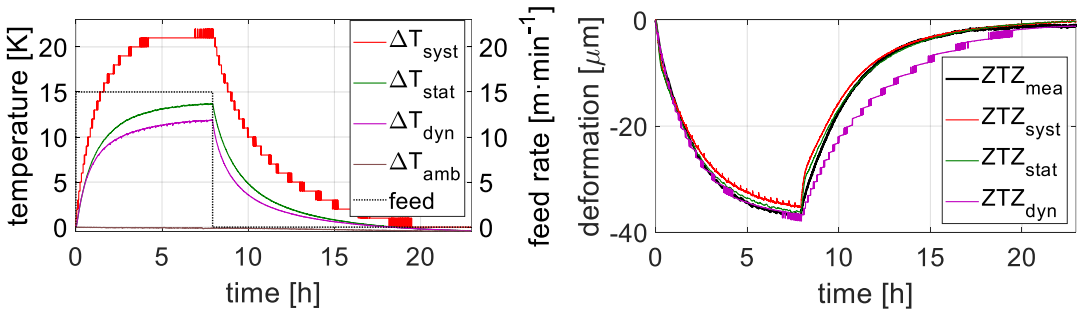

Fig. 34 Behaviours of measured temperatures and Z-axis feed rate (left) and behaviours of measured and simulated deformations in the Z direction (right) during test No. 2c.

An evaluation of the approximation quality of applied compensation models on verification measurements is presented in Table 4. The *FIT* and *PTP* methods are used. The *PTP* value is evaluated using the *PTP* of measured and residual (*RES)* deformations.

Table 4 Evaluation of the approximation quality for verification tests.

Thermal error model	5 m·min^{-1}			15 m·min^{-1}		
	PTP [µm]		*FIT*	*PTP* [µm]		*FIT*
	Mea.	RES	[%]	Mea.	RES	[%]
XTY_{syst}	4,4	3,8	0	3,2	7	0
XTY_{stat}	4,4	3,6	0	3,2	5,7	0
XTY_{dyn}	4,4	3,5	0	3,2	5,3	0
XTZ_{syst}	9,2	3	63	19,7	4,2	35
XTZ_{stat}	9,2	3	54	19,7	3,4	52
XTZ_{dyn}	9,2	2,9	62	19,7	2,9	72
YTY_{syst}	5,1	4,4	0	28,8	23,7	21
YTY_{stat}	5,1	4,3	0	28,8	23,7	21
YTY_{dyn}	5,1	4,4	0	28,8	24,1	18
YTZ_{syst}	12,4	4,4	69	36,9	5,2	83
YTZ_{stat}	12,4	4	75	36,9	4,1	76
YTZ_{dyn}	12,4	3,8	75	36,9	4	66
ZTY_{syst}	8,4	3,1	46	15,5	14,4	33
ZTY_{stat}	8,4	3,1	43	15,5	14,1	36
ZTY_{dyn}	8,4	3	49	15,5	13,3	38
ZTZ_{syst}	16,4	4,7	46	37	3	94
ZTZ_{stat}	16,4	3,2	43	37	3,6	91
ZTZ_{dyn}	16,4	3	52	37	4,6	83

From the presented results, it can be seen that for motion in the direction of the MT linear axis Y, it is unnecessary to compensate for thermal error in the X direction (XTY) because of its small size (small effect on the production accuracy). For motion in the direction of the MT linear axis Z, the prediction of thermal error in the X direction (XTZ) has a better approximation quality of the cooling phase for the T_{syst} input and the prediction of thermal error in the Z direction (ZTZ) has a better approximation of the cooling phase with the T_{stat} or T_{dyn} input. In general, it is not possible to determine which temperature input is the most suitable in terms of the approximation quality. However, it can be stated that the basic input Tsyst is not significantly worse (in terms of approximation quality) in predicting the TCP displacement (in the heating phase) than the additional temperature inputs T_{stat} and T_{dyn} (in some cases can provide better prediction quality; these cases cannot be generalised).

5 Portability of the thermal error compensation model

This chapter focuses on the portability of thermal compensation models to other MTs of the same (or very similar) type and size. The motivation for using one compensation model across the MT production line is to save resources in the product finishing phase, e.g., reduction of time necessary to calibration measurements, modelling effort, simplification of model implementation into control system etc. Creating a new thermal compensation model is challenging and extensive, as shown in the previous chapter. It is necessary to perform many time-consuming measurements on the finished MT to thermal compensation model successful development and verification. Transfer of a thermal error compensation model structure (with a simple adjustment of model parameters) results in time-saving for the MT producer in the finishing phase before the expedition to a customer.

Based on the previous paragraph was decided that a portability rating would be done by sorting the models into three basic groups:

- Portable without correction of model parameters
- Portable with necessary corrections
- Non-portable (need to build up an entirely new model)

5.1 Target machines

Additional sets of measurements from the other 3 MTs of the same product line were provided for the thesis purposes. The MTs are 5-axis milling centres of the upper gantry type as well (basic structure of the MT shown in Fig. 12). At first glance, the MTs differ only in the serial number (further in short S/N): 138, 118, 103, and 79. Please note that the compensation model introduced in chapter 4 was calibrated on

the target machine 138. However, there are some differences between the target machines with direct or indirect impacts on thermal issues. The differences are summarised in Table 5. There are differences between the target MTs in preload of the ball screws, the lubrication used, the cooling of the motion axes, the placement of MTs, and periods of measurements. The target machine 138 is used for the production (however, in a laboratory) similarly to the target machine 118. Target machines 103 and 79 were placed in similar MT producer's show rooms and regarded as brand new. The target machine 118 is placed in a common production hall.

Table 5 Description of target machines differences.

<table>
<tr><th>MT</th><th>Preload of Y and Z axis ball-screws [kN]</th><th>Lubricant for axes</th><th>Cooling of feed drives</th><th>Placement</th><th>Date of experiments</th></tr>
<tr><td>138</td><td>2,1</td><td rowspan="2">NLGI 00</td><td>12 kW (spindle and A axis – compressor cooler)</td><td>Laboratory</td><td>2021/03</td></tr>
<tr><td>118</td><td rowspan="3">1,7</td><td rowspan="3">8 kW (A axis – compressor cooler), 0.56 kW/K (spindle – surge cooler)</td><td>Production hall</td><td>2019/07</td></tr>
<tr><td>103</td><td>Show room</td><td>2019/06</td></tr>
<tr><td>79</td><td>ISO VG 100</td><td>Show room</td><td>2015/07</td></tr>
</table>

Measurements from a 5-axis MT of similar size to the target machines 138, 118, 103, and 79 but different producer (in short AMP, *another machine producer*) are also available, with the MT differ a little by the structure and kinematics of the motion axes (see Fig. 35 for more detail).

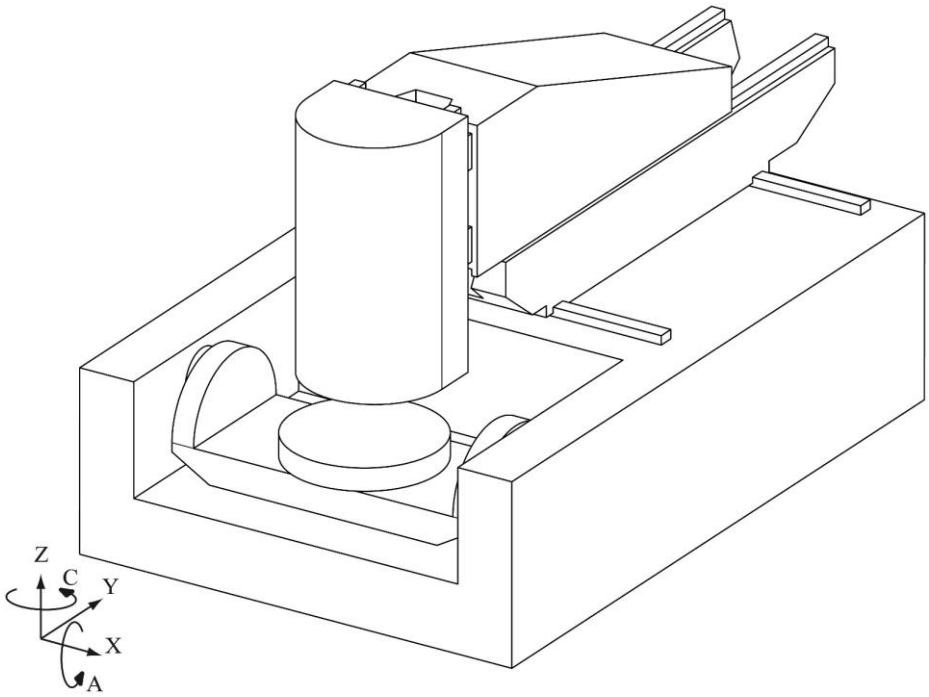

Fig. 35 Schema of basic structures of the target machine by AMP.

5.2 Measurement set-ups

All measurements listed here were performed similarly to the target machine 138 as described in section 4.1.2. Compared to the target machine 138, the other MTs were not identically sensory equipped. Table 6 shows the differences in the sensor placements of each target machine. A full black circle means that the MT is equipped with the specified sensor. Otherwise, an outlined white circle is shown in the case the MT is not equipped with a specific sensor.

Table 6 Differences in the equipment of target machines with temperature sensors.

MT / sensor	S/N 138	S/N 118	S/N 103	S/N 79	AMP
T_{syst}	●	●	●	●	●
T_{stat}	●	●	●	○	●
T_{dyn} at motion in Y-axis tests	●	●	●	○	●
T_{dyn} at motion in Z-axis tests	●	○	○	○	●

The following table contains all experiments performed and used to evaluate the portability of the thermal compensation model.

Table 7 Performed experiments for all target machines used for portability examination.

No.	MT	Inspected thermal error	Heat source	Feed rate [m·min^{-1}]
3	79	XTY, YTY, ZTY	Y feed drive	15
4	79	XTZ, YTY, ZTZ	Z feed drive	15
5	103	XTY, YTY, ZTY	Y feed drive	8
6	103	XTZ, YTY, ZTZ	Z feed drive	8
7	118	XTY, YTY, ZTY	Y feed drive	15
8	118	XTZ, YTY, ZTZ	Z feed drive	15
9	AMP	XTY, YTY, ZTY	Y feed drive	8
10	AMP	XTZ, YTY, ZTZ	Z feed drive	8

5.3 Inspection of portability of thermal error compensation model

The portability of the thermal compensation model developed on the target machine 138 will be evaluated in this section. The compensation model is specific for the three different temperature inputs regarding the approximation of movements in Y and Z MT linear axes. It is possible to continue evaluating the influence of the used inputs on the approximation quality in the case of another target machines.

The approximation quality (or model efficiency in other words) is evaluated using the FIT and PTP methods (introduced in section 4.2) and additionally by a magnification of the model by correction factors. The correction factor is determined by comparing the measured and simulated deformation values at the end of the heating phase. In other words, if the simulated deformation vector is multiplied by the correction factor, the value of the new corrected simulated deformation vector will be equal to the measured vector at the end of the heating phase.

Calculations of simulated deformations for specific directions, temperature inputs, tests, and with the correction factor (g) applied are given in equations

(17) to (22), where *in* = syst (T_{syst}), stat (T_{stat}), dyn (T_{dyn}); *S/N = a serial number of measured target machine; 138 =* the serial number of target machine used for compensation model build-up.

$$_{138}XTY_{in}^{S/N} = \Delta T_{in} \cdot \varepsilon_{in}^{XTY} \cdot g_{in}^{S/N} \quad (17)$$

$$_{138}XTZ_{in}^{S/N} = \Delta T_{in} \cdot \varepsilon_{in}^{XTZ} \cdot g_{in}^{S/N} \quad (18)$$

$$_{138}YTY_{in}^{S/N} = \Delta T_{in} \cdot \varepsilon_{in}^{YTY} \cdot g_{in}^{S/N} \quad (19)$$

$$_{138}YTY_{in}^{S/N} = \Delta T_{in} \cdot \varepsilon_{in}^{YTY} \cdot g_{in}^{S/N} \quad (20)$$

$$_{138}ZTY_{in}^{S/N} = \left((\Delta T_{in} - \Delta T_{amb}) \cdot \varepsilon_{in}^{ZTY} + \underbrace{\Delta T_{amb} \cdot \varepsilon_{amb}}_{Z_{amb}} \right) \cdot g_{in}^{S/N} \quad (21)$$

$$_{138}ZTZ_{in}^{S/N} = \left((\Delta T_{in} - \Delta T_{amb}) \cdot \varepsilon_{in}^{ZTZ} + \underbrace{\Delta T_{amb} \cdot \varepsilon_{amb}}_{Z_{amb}} \right) \cdot g_{in}^{S/N} \quad (22)$$

The complete graphical outputs from applying the compensation models on the measured data are presented in Annex 2. Selected graphs with significant outcomes are also used in chapter 6 at the end of the thesis to support discussed results.

Table 8 shows the correction factors per individual temperature inputs for each target machine. Unavailable measurements (the temperature inputs were missing) are signed with "x". The measurements where the correction factor could not be determined are signed by "-".

Table 8 Correction factors ($g_{in}^{S/N}$) for defined temperature inputs of each target machine for the model build-up on the target machine S/N 138.

Thermal error model	S/N of the target machine											
	79			103			118			AMP		
	Input temperature (T_{in})											
	T_{syst}	T_{stat}	T_{dyn}	T_{syst}	T_{stat}	T_{dyn}	T_{syst}	T_{stat}	T_{dyn}	T_{syst}	T_{stat}	T_{dyn}
${}_{138}XTY_{in}^{S/N}$	1,71	x	x	3,1	5,35	3,1	-	-	-	1,27	1,16	1,09
${}_{138}XTZ_{in}^{S/N}$	1,5	x	x	2,25	2,86	x	1,66	2	x	0,3	0,24	0,28
${}_{138}YTY_{in}^{S/N}$	3,34	x	x	4,29	5,7	4,74	-	-	-	-	-	-
${}_{138}YTZ_{in}^{S/N}$	1,12	x	x	1,33	1,7	x	-	-	x	4,83	4,06	4,88
${}_{138}ZTY_{in}^{S/N}$	1,2	x	x	1,72	2,84	1,69	1,89	2,74	2,8	0,89	1,2	1,34
${}_{138}ZTZ_{in}^{S/N}$	0,8	x	x	0,85	1,05	x	1,7	2,08	x	0,93	0,78	0,91

Table 9 (for target machines 79, 108) and Table 10 (for target machines 118, AMP) show the results of the approximation quality evaluation by the *FIT* method. The assessment was performed both for the uncorrected model application (columns named "N") and for the simulated deformation by the adjusted model with the help of correction factor (columns named "C"). Please note that only the heating phases are considered in the evaluation.

Table 9 Results of the approximation quality evaluation by the FIT method for target machines 79, 103 for the model build-up on the target machine S/N 138.

Thermal error model	S/N of the target machine							
	79		103					
	Input temperature (T_{in})							
	T_{syst}		T_{syst}		T_{stat}		T_{dyn}	
	N	C	N	C	N	C	N	C
${}_{138}XTY_{in}^{S/N}$	0	0	0	0	0	0	0	25
${}_{138}XTZ_{in}^{S/N}$	5	38	0	57	0	66	x	x
${}_{138}YTY_{in}^{S/N}$	0	0	0	0	0	0	0	0
${}_{138}YTZ_{in}^{S/N}$	24	0	16	77	0	77	x	x
${}_{138}ZTY_{in}^{S/N}$	40	63	0	56	0	50	0	33
${}_{138}ZTZ_{in}^{S/N}$	27	89	47	87	81	90	x	x

Table 10 Results of the approximation quality evaluation by the FIT method for target machines 118, AMP for the model build-up on the target machine S/N 138.

Thermal error model	S/N of the target machine											
	118						AMP					
	Input temperature (T_{in})											
	T_{syst}		T_{stat}		T_{dyn}		T_{syst}		T_{stat}		T_{dyn}	
	N	C	N	C	N	C	N	C	N	C	N	C
${}_{138}XTY_{in}^{S/N}$	-	-	-	-	-	-	0	0	0	0	4	4
${}_{138}XTZ_{in}^{S/N}$	20	47	0	73	x	x	0	0	0	0	0	0
${}_{138}YTY_{in}^{S/N}$	-	-	-	-	-	-	-	-	-	-	-	-
${}_{138}YTZ_{in}^{S/N}$	-	-	-	-	x	x	0	69	0	63	0	60
${}_{138}ZTY_{in}^{S/N}$	0	48	0	44	0	24	27	14	12	21	0	2
${}_{138}ZTZ_{in}^{S/N}$	28	53	2	65	x	x	5	0	0	0	0	0

Table 11 (for target machines 79, 108) and Table 12 (for target machines 118, AMP) show the results of the approximation quality evaluation by the *PTP* method. There are always 2 numbers in table cells: the upper number represents the PTP value of the measured deformation, the lower value represents the PTP value of the residual deformation.

Table 11 Results of the approximation quality evaluation by the PTP method for target machines 79, 103 for the model build-up on the target machine S/N 138.

Thermal error model	S/N of the target machine							
	79		103					
	Input temperature (T_{in})							
	T_{syst}		T_{syst}		T_{stat}		T_{dyn}	
	N	C	N	C	N	C	N	C
${}_{138}XTY_{in}^{S/N}$	7,9 7,2	7,9 10,2	8,4 5,8	8,4 6,6	8,4 6,9	8,4 3,7	8,4 5,7	8,4 4
${}_{138}XTZ_{in}^{S/N}$	34,5 17,7	34,5 16,8	28,3 16	28,3 8,8	28,3 18,6	28,3 8,5	x	x
${}_{138}YTY_{in}^{S/N}$	17,5 15,3	17,5 23,6	10,7 8,9	10,7 8,8	10,7 9,2	10,7 7,1	10,7 9	10,7 8,9
${}_{138}YTZ_{in}^{S/N}$	57,9 37,9	57,9 43	24,6 8,6	24,6 5,2	24,6 10,7	24,6 3,7	x	x
${}_{138}ZTY_{in}^{S/N}$	23,6 5,6	23,6 6	15,7 6,6	15,7 4,8	15,7 10,2	15,7 4,6	15,7 7	15,7 5,7
${}_{138}ZTZ_{in}^{S/N}$	32,5 10,4	32,5 3,9	17 5,3	17 3,2	17 1,8	17 2	x	x

Table 12 Results of the approximation quality evaluation by the PTP method for target machines 118, AMP for the model build-up on the target machine S/N 138.

Thermal error model	S/N of the target machine											
	118						AMP					
	Input temperature (T_{in})											
	T_{syst}		T_{stat}		T_{dyn}		T_{syst}		T_{stat}		T_{dyn}	
	N	C	N	C	N	C	N	C	N	C	N	C
${}_{138}XTY_{in}^{S/N}$	-	-	-	-	-	-	9,7 11,2	9,7 11,2	9,7 9,6	9,7 9,6	9,7 9,4	9,7 9,4
${}_{138}XTZ_{in}^{S/N}$	37,8 20,7	37,8 12,3	37,8 21,7	37,8 8,7	x	x	8,7 16,6	8,7 6,9	8,7 19,2	8,7 6,5	8,7 16,1	8,7 6,6
${}_{138}YTY_{in}^{S/N}$	-	-	-	-	-	-	-	-	-	-	-	-
${}_{138}YTZ_{in}^{S/N}$	-	-	-	-	x	x	117,7 94,2	117,7 30,2	117,7 90,5	117,7 23,7	117,7 94,6	117,7 21,5
${}_{138}ZTY_{in}^{S/N}$	38 19,6	38 11,3	38 25,4	38 11,4	38 25,3	38 15,1	10,3 7,7	10,3 7,7	10,3 6,9	10,3 6,7	10,3 7,7	10,3 7,7
${}_{138}ZTZ_{in}^{S/N}$	59,7 27,3	59,7 17	59,7 31	59,7 14,5	x	x	27,1 12,7	27,1 11,5	27,1 17,4	27,1 12,7	27,1 15,4	27,1 13,7

5.3.1 Results

The division of the models into 3 basic groups was established in terms of their portability evaluation at the beginning of chapter 5. The results are summarised in Table 13. The portability efficiency of the model to the AMP MT was not considered in Table 13. The portability of the thermal error compensation model between different MT producers is not (and probably never will be) a real practice. However, surprisingly high approximation quality in ZTY and ZTZ seems to be the good results, may be the result of chance.

The model has to meet the requirement of correction factor equal to 1±0.1, *FIT* greater than 80 %, and *PTP* of measured deformation greater than *PTP* of simulated deformation (by uncorrected model) to be included in the resulting group "Portable without correction". The simulated deformation has to follow a curve of the same order as the measured deformation, and it can be proved by *FIT* and *PTP* methods.

The model with correction factor less than 0.33 or with correction factor greater than 3 or with *FIT* less than 20 % (for corrected model) or with *PTP* of

measured deformation less than *PTP* of simulated deformation (by corrected model) was included in the resulting group "Non-portable".

Table 13 The resulting evaluation of the portability of each compensation model for each target machine and temperature input.

Motion in linear axis	Portable without correction	Portable with necessary correction	Non-portable
Y	-	${}_{138}ZTY_{syst}^{79}$ ${}_{138}ZTY_{syst}^{103}$ ${}_{138}ZTY_{syst}^{118}$ ${}_{138}ZTY_{stat}^{103}$ ${}_{138}ZTY_{stat}^{118}$ ${}_{138}ZTY_{dyn}^{103}$ ${}_{138}ZTY_{dyn}^{118}$	${}_{138}XTY_{syst}^{79}$ ${}_{138}XTY_{syst}^{103}$ ${}_{138}XTY_{syst}^{118}$ ${}_{138}XTY_{stat}^{103}$ ${}_{138}XTY_{stat}^{118}$ ${}_{138}XTY_{dyn}^{103}$ ${}_{138}XTY_{dyn}^{118}$ ${}_{138}YTY_{syst}^{79}$ ${}_{138}YTY_{syst}^{103}$ ${}_{138}YTY_{syst}^{118}$ ${}_{138}YTY_{stat}^{103}$ ${}_{138}YTY_{stat}^{118}$ ${}_{138}YTY_{dyn}^{103}$ ${}_{138}YTY_{dyn}^{118}$
Z	${}_{138}ZTZ_{stat}^{103}$	${}_{138}XTZ_{syst}^{79}$ ${}_{138}XTZ_{syst}^{103}$ ${}_{138}XTZ_{syst}^{118}$ ${}_{138}XTZ_{stat}^{103}$ ${}_{138}XTZ_{stat}^{118}$ ${}_{138}YTZ_{syst}^{103}$ ${}_{138}YTZ_{stat}^{103}$ ${}_{138}ZTZ_{syst}^{79}$ ${}_{138}ZTZ_{syst}^{103}$ ${}_{138}ZTZ_{syst}^{118}$ ${}_{138}ZTZ_{stat}^{118}$	${}_{138}YTZ_{syst}^{79}$ ${}_{138}YTZ_{syst}^{118}$ ${}_{138}YTZ_{stat}^{118}$

6 Summary and discussion

The inputs to the introduced thermal compensation models are measured temperatures. The choice of a suitable temperature input is important for the approximation quality of the simulated thermal error. The research was conducted to compensate for the thermal errors caused by motion in the MT linear axes Y and Z (movement in the X-axis was not considered in the thesis to reduce the breadth of work). The target machines were 5-axis milling centres of the upper gantry type. The MTs are standardly equipped with temperature sensors in the feed drive motors for diagnostic purposes (T_{syst}). The MTs were further equipped with additional temperature sensors T_{stat} (placed on the bearing houses of the ball screw bearings) and T_{dyn} (placed on the front sides of the ball screw nuts).

Thermal error compensation models based on the principle of transfer functions were calibrated on measurements at a feed rate of 10 $m \cdot min^{-1}$. Only the heating phases (caused by motion linear axis activity) were considered for modelling. All considered temperature inputs into models showed similar approximation quality during the calibration measurement and identification process. The model dealing with changes in the MT environment was successfully calibrated only for the Z direction.

Measurements at feed rates of 5 and 15 $m \cdot min^{-1}$ were performed to verify the linearity of the calibrated models. No significant differences in the approximation quality of the thermal error models have been observed within different temperature inputs during the heating phases. The worse approximation quality was determined for XTY and YTY thermal errors. The thermal error XTY was minimal compared to the others, and no compensation was applied. The temperature input T_{syst} reached a similar approximation quality to thermal error predictions with temperature inputs T_{stat} and T_{dyn}. This could be essential information for MT producers. It was not possible to unequivocally determine the most suitable temperature input for accurate prediction of the thermal error from the results.

Interesting differences between the considered temperature inputs were noticed during the cooling phases of experiments. However, the evaluation of the cooling phase is not the main aim of this thesis; there could be interesting insights for future research, e.g., the compensation model with the temperature input T_{syst} reaches a better approximation quality for XTZ error (see Fig. 36) and contrary, the temperature inputs T_{stat} or T_{dyn} for ZTZ (see Fig. 37).

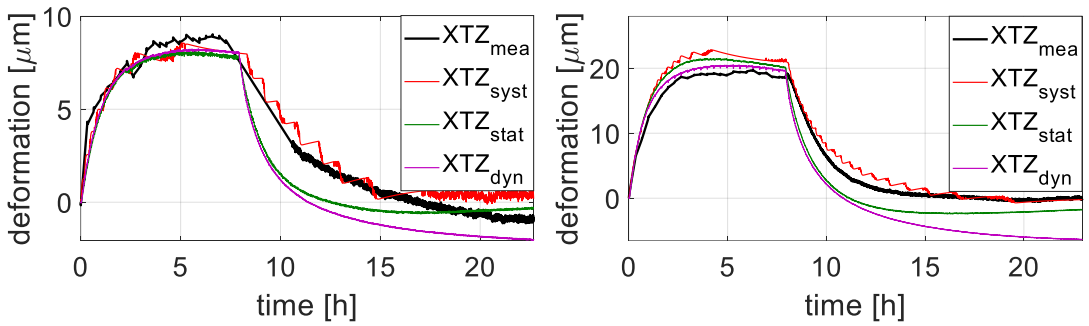

Fig. 36 Behaviours of measured and simulated deformations in the X direction during tests No. 2b (left) and No. 2c (right).

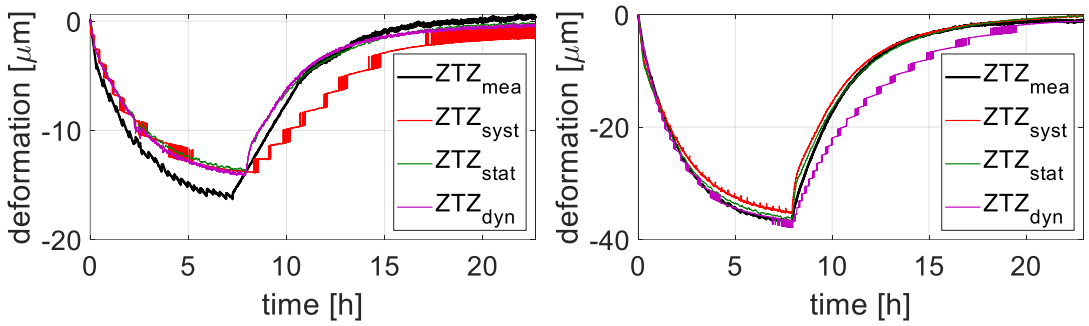

Fig. 37 Behaviours of measured and simulated deformations in the Z direction during tests No. 2b (left) and No. 2c (right).

A "universal" and portable without corrections compensation model for all MTs of the same product line would be the best solution for MT producers. However, this is not possible due to manufacturing and assembly inaccuracies, MT surrounding, thermal behaviour changes during the life cycle of the MT related to wear and tear etc. A portable compensation model with simple corrections (with the help of output gain) would be a more realistic and also useful solution for the MT producer. In this case, it would not be necessary to develop an original compensation model for each

MT. Only necessary verification (or tuning) cycles would be performed on each new MT to determine the correction factors.

The evaluations of compensation model portability were performed. Compensation models developed on one target machine (S/N138) were evaluated. The evaluation was performed for the other 3 MTs of the same product line and 1 MT of similar structure and size from another MT producer. Please note that the AMP machine was added to the research out of sheer interest (and data were available); such possibility (to transfer models between different manufacturers) has no basis in reality.

Models with a simulated curve of a different order than the measured deformation were evaluated as non-transferable. Most models were considered as transferable with simple correction. The results reflected manufacturing and assembly inaccuracies, different ball screws preload, different lubrication, MT placement, different MT age and wear. MT from another MT producer achieved surprisingly high approximation quality in ZTZ thermal errors. This may indicate possible similar thermal behaviour of similar-sized structures (could also be the result of chance).

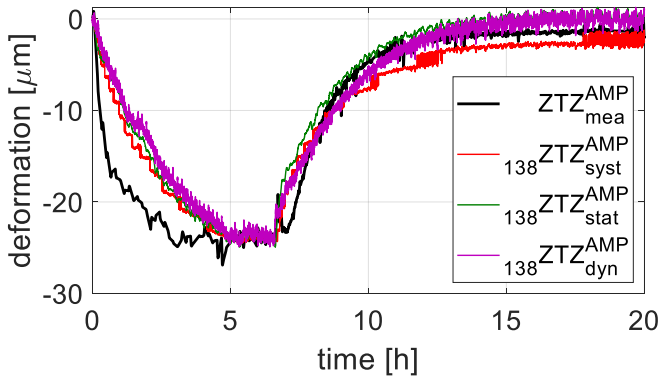

Fig. 38 Behaviours of measured and simulated deformations (by corrected models) in Z direction during test No. 10.

The results concerning the portability also confirm the previous presumption of the temperature input T_{syst}. This temperature input has a similar potential as the

additional temperature inputs T_{stat} and T_{dyn}. Therefore, the use of additional temperature inputs makes sense, especially for producers of higher-precision MTs where the possibility to choose the best temperature input describing the thermal behaviour of the MT could be beneficial despite the additional cost.

Further research on the portability of compensation models of thermal errors caused by motion in linear axes should focus on the inclusion of the cooling phases into their structure. A major challenge will be to consider a real cutting process. Focus on the long-term stability of the models (e.g., by a combination of direct and indirect compensation methods) is also very important.

7 Conclusions

Chapter 3 presents state of the art – namely, the deformation of MTs, heat generation and its transfer in MT, and thermal error. There are several options to reduce the size of the thermal error – reduction of changes in the temperature field of the MT, reduction of the MT's sensitivity to changes in the temperature field, or compensation of the thermal errors. In this thesis, a compensation approach is used. Therefore, different approaches and methods of compensation are described. The input to the thermal compensation function is usually temperature, and the output is deformation. For calibration of the thermal compensation function, knowledge of both input and output is required. Thus, methods and conditions of measuring the input-output variables have been described.

In Chapter 4, an evaluation of the influence of different input variables (to the calibrated thermal compensation models based on the transfer function principle) on the approximation quality of the simulated thermal error was performed. The temperatures embedded in the feed drive motors, on the bearings houses of the ball screw bearing, and on the front sides of the ball screw nuts were used. The evaluation was performed for motion in the linear Y and Z axes and the heating phase only. No significant difference was found between the different temperature inputs in terms of the approximation quality.

In Chapter 5, an evaluation of the portability of the thermal compensation models developed on the target machine described in the previous chapter was performed. The evaluation was realised on 4 MTs of the same product line and 1 MT of similar size and structure by another MT producer. Most of the compensation models are portable completely or with simple correction on other target machines. Other compensation models were considered as non-portable due to the different thermal behaviour among the tested MTs. The results were further discussed in more detail.

Finally, possibilities of future research on the portability of thermal error compensation models were introduced. Successful completion of the research could bring considerable time and resources savings to MT producers.

Lists

List of references

[1] MAYR, Josef, Jerzy JEDRZEJEWSKI, Eckart UHLMANN, M. ALKAN DONMEZ, Wolfgang KNAPP, Frank HÄRTIG, Klaus WENDT, Toshimichi MORIWAKI, Paul SHORE, Robert SCHMITT, Christian BRECHER, Timo WÜRZ a Konrad WEGENER. Thermal issues in machine tools. *CIRP Annals* [online]. 2012, **61**(2), 771–791. ISSN 0007-8506. Avaible online: doi:10.1016/j.cirp.2012.05.008

[2] BÁRTA, P. *Frekvenční přenosové funkce v termomechanice*. Praha: Disertační práce, ČVUT v Praze, Fakulta strojní, Ústav mechaniky tekutin a energetiky. 2008

[3] RAMESH, R, M.A MANNAN a Aun-Neow POO. Error compensation in machine tools — a review: Part I: geometric, cutting-force induced and fixture-dependent errors. *International Journal of Machine Tools and Manufacture*. 2000, 1235–1256.

[4] HOUŠA, J. *Stavba výrobních strojů 2*. Praha: Vydavatelství ČVUT, 1984.

[5] BRYAN, J. International Status of Thermal Error Research (1990). *CIRP Annals* [online]. 1990, **39**(2), 645–656. ISSN 0007-8506. Avaible online: doi:10.1016/S0007-8506(07)63001-7

[6] WECK, M., P. MCKEOWN, R. BONSE a U. HERBST. Reduction and Compensation of Thermal Errors in Machine Tools. *CIRP Annals* [online]. 1995, **44**(2), 589–598. ISSN 0007-8506. Avaible online: doi:10.1016/S0007-8506(07)60506-X

[7] WECK, Manfred. *Handbook of Machine Tools: Metrological analysis and performance tests*. Wiley, 1984. ISBN 978-0-471-26225-1.

[8] BORSKÝ, Václav. *Základy stavby obráběcích strojů*. Nakladatelství VUT Brno. 1991.

[9] JEDRZEJEWSKI, J. Directions for Improving the Thermal Stability of Machine Tools. 1998, Chicago: ASME, 165–182.

[10] ISO 230-3:2020. Test code for machine tools — Part 3: Determination of thermal effects. *ISO* [online]. Avaible online: https://www.iso.org/cms/render/live/en/sites/isoorg/contents/data/standard/07/32/73291.html

[11] BERGMAN, Theodore L., Frank P. INCROPERA, Adrienne S. LAVINE a David P. DEWITT. *Introduction to Heat Transfer*. John Wiley & Sons, 2011. ISBN 978-0-470-50196-2.

[12] HERBST, Uwe. *Analyse und Kompensation thermoelastischer Verlagerungen*. Shaker, 2002. ISBN 978-3-8322-0298-9.

[13] MADHUSUDANA, C. V. Accuracy in thermal contact conductance experiments - the effect of heat losses to the surroundings. *International Communications in Heat and Mass Transfer* [online]. 2000, **27**(6), 877–891. ISSN 0735-1933. Avaible online: doi:10.1016/S0735-1933(00)00168-8

[14] RAMESH, R, M. A MANNAN a A. N POO. Error compensation in machine tools — a review: Part II: thermal errors. *International Journal of Machine Tools and Manufacture* [online]. 2000, **40**(9), 1257–1284. ISSN 0890-6955. Avaible online: doi:10.1016/S0890-6955(00)00010-9

[15] GROSSMANN, Knut, ed. *Thermo-energetic Design of Machine Tools: A Systemic Approach to Solve the Conflict Between Power Efficiency, Accuracy and Productivity Demonstrated at the Example of Machining Production* [online]. Springer International Publishing, 2015. Lecture Notes in Production Engineering. ISBN 978-3-319-12624-1. Avaible online: doi:10.1007/978-3-319-12625-8

[16] MIAN, Naeem S. *Efficient machine tool thermal error modelling strategy for accurate offline assessment* [online]. 2010. University of Huddersfield. Avaible online: http://eprints.hud.ac.uk/id/eprint/11054/

[17] PUTZ, Matthias, Carsten RICHTER, Joachim REGEL a Michael BRÄUNIG. Industrial relevance and causes of thermal issues in machine tools. In: . 2018.

[18] HORÁK, K. *Kompenzace teplotně způsobených úhlových deformací obráběcích strojů pomocí Peltierových článků*. ČVUT v Praze. 2012

[19] DONMEZ, M. A., M. H. HAHN a J. A. SOONS. A Novel Cooling System to Reduce Thermally-Induced Errors of Machine Tools. *CIRP Annals* [online]. 2007, **56**(1), 521–524. ISSN 0007-8506. Avaible online: doi:10.1016/j.cirp.2007.05.124

[20] HOREJŠ, O. a další. *Závěrečná zpráva projektu 1.4.2 za rok 2009.* V-09-032. Praha: VCSVTT. 2009

[21] HELLMICH, Arvid, Janine GLÄNZEL a Alexander PIERER. Analyzing and Optimizing the Fluidic Tempering of Machine Tool Frames. In: . 2018.

[22] LAŠOVÁ, Václava. *KKS/ZSVS základy stavby obráběcích strojů* [online]. Západočeská univerzita v Plzni, 2012. ISBN 978-80-261-0126-0. Avaible online: http://dspace5.zcu.cz/handle/11025/16835

[23] HOOIJKAMP, E. C. a F. van KEULEN. Topology optimization for linear thermo-mechanical transient problems: Modal reduction and adjoint sensitivities. *International Journal for Numerical Methods in Engineering* [online]. 2018, **113**(8), 1230–1257. ISSN 1097-0207. Avaible online: doi:https://doi.org/10.1002/nme.5635

[24] ALEXANDR, Kozačok. Analýza teplotních deformací nosné struktury stroje a návrh optimalizačních úprav [online]. 2013. Avaible online: https://dspace.cvut.cz/handle/10467/19827

[25] TUREK, P., J. JĘDRZEJEWSKI a W. MODRZYCKI. Methods of machine tool error compensation. *Journal of Machine Engineering* [online]. 2010, **Vol. 10, No. 4**. ISSN 1895-7595. Avaible online: http://yadda.icm.edu.pl/baztech/element/bwmeta1.element.baztech-8823716c-580b-404e-adb2-86a9e908aa06

[26] BRECHER, C., P. HIRSCH a M. WECK. Compensation of Thermo-elastic Machine Tool Deformation Based on Control internal Data. *CIRP Annals* [online]. 2004, **53**(1), 299–304. ISSN 0007-8506. Avaible online: doi:10.1016/S0007-8506(07)60702-1

[27] MAYR, Josef, Philip BLASER, Adrian RYSER a Pablo HERNANDEZ-BECERRO. An adaptive self-learning compensation approach for thermal errors on 5-axis machine tools handling an arbitrary set of sample rates. *CIRP Annals* [online]. 2018, **67**(1), 551–554. ISSN 0007-8506. Avaible online: doi:10.1016/j.cirp.2018.04.001

[28] HOREJŠ, Otakar, Martin MARES a Lukáš NOVOTNÝ. Advanced Modelling of Thermally Induced Displacements and Its Implementation into Standard CNC Controller of Horizontal Milling Center. *Procedia CIRP* [online]. 2012, **4**, 67–72. Avaible online: doi:10.1016/j.procir.2012.10.013

[29] LI, Yang, Wanhua ZHAO, Shuhuai LAN, Jun NI, Wenwu WU a Bingheng LU. A review on spindle thermal error compensation in machine tools. *International Journal of Machine Tools and Manufacture* [online]. 2015, **95**, 20–38. ISSN 0890-6955. Avaible online: doi:10.1016/j.ijmachtools.2015.04.008

[30] NAUMANN, Christian, Janine GLÄNZEL a Matthias PUTZ. Comparison of basis functions for thermal error compensation based on regression analysis – a simulation based case study. *Journal of Machine Engineering* [online]. 2020, **20**, 28–40. Avaible online: doi:10.36897/jme/128629

[31] LIU, Quan, Junwei YAN, D. PHAM, Zude ZHOU, Wenjun XU, Qin WEI a Chunqian JI. Identification and optimal selection of temperature-sensitive measuring points of thermal error compensation on a heavy-duty machine tool. *The*

International Journal of Advanced Manufacturing Technology [online]. 2016, **85**. Avaible online: doi:10.1007/s00170-015-7889-1

[32] HERNÁNDEZ BECERRO, Pablo, Josef MAYR, Philip BLASER, Florentina PAVLIČEK a Konrad WEGENER. Model order reduction of thermal models of machine tools with varying boundary conditions. In: *1st Conference on Thermal Issues in Machine Tools*: *Conference on Thermal Issues in Machine Tools: Proceedings* [online]. B.m.: Verlag Wissenschaftliche Scripten, 2018, s. 169–178. ISBN 978-3-95735-085-5. Avaible online: https://www.research-collection.ethz.ch/handle/20.500.11850/311793

[33] KOHÚT, P., Otakar HOREJŠ a Martin MAREŠ. Machine Tool Heat Transfer FEA and Experimental Identification of Convective Heat Transfer. *MM Science Journal*. 2012.

[34] BÁRTA, P. Modelování teplotních a teplotně-mechanických jevů tepelnými přenosovými funkcemi. *Praha : VCSVTT*. 2007.

[35] URIARTE, L. *Thermal Modal Analysis*. Proceedings SIG meeting on Thermal Issues in Precision Engineering, Eindhoven. 2006

[36] ISO 230-3 Test code for machine tools - Part 3: Determination of thermal effects. International Organization for Standardization ISO, Geneva, Switzerland, 2007, p. 44.

[37] BRECHER, Christian a Adam WISSMANN. *Stressing unit for modelling of thermal behaviour of a milling machine* [online]. RWTH-CONV-171968. B.m.: Unibertsitatea Zerbitzu Editoriala. 2009. Avaible online: doi:910008674

[38] CHEN, Jenq-Shyong. A study of thermally induced machine tool errors in real cutting conditions. *International Journal of Machine Tools and Manufacture* [online]. 1996, **36**(12), 1401–1411. ISSN 0890-6955. Avaible online: doi:10.1016/0890-6955(95)00096-8

[39] HOREJŠ, Otakar a Martin MARES. REAL-TIME COMPENSATION OF MACHINE TOOL THERMAL ERRORS INCLUDING CUTTING PROCESS. *Journal of Machine Engineering*. 2015, **15**, 5–18.

[40] MAREŠ, Martin a Otakar HOREJŠ. Modelling of Cutting Process Impact on Machine Tool Thermal Behaviour Based on Experimental Data. *Procedia CIRP* [online]. 2017, **58**, 16th CIRP Conference on Modelling of Machining Operations (16th CIRP CMMO), 152–157. ISSN 2212-8271. Avaible online: doi:10.1016/j.procir.2017.03.208

[41] BLASER, P., Josef MAYR a Konrad WEGENER. LONG-TERM THERMAL COMPENSATION OF 5-AXIS MACHINE TOOLS DUE TO THERMAL ADAPTIVE

LEARNING CONTROL. *MM Science Journal* [online]. 2019, 3164–3171. Avaible online: doi:10.17973/MMSJ.2019_11_2019066

[42] MAREŠ, Martin, Otakar HOREJŠ a Lukáš HAVLÍK. Thermal error compensation of a 5-axis machine tool using indigenous temperature sensors and CNC integrated Python code validated with a machined test piece. *Precision Engineering* [online]. 2020, **66**, 21–30. ISSN 0141-6359. Avaible online: doi:10.1016/j.precisioneng.2020.06.010

[43] STRATEGY OF MILLING CENTER THERMAL ERROR COMPENSATION USING A TRANSFER FUNCTION MODEL AND ITS VALIDATION OUTSIDE OF CALIBRATION RANGE | MM Science Journal. *www.mmscience.eu* [online]. Avaible online: https://www.mmscience.eu/journal/issues/november-2019/articles/strategy-of-milling-center-thermal-error-compensation-using-a-transfer-function-model-and-its-validation-outside-of-calibration-range

[44] STRAKA, Michal a Martin MAREŠ. Portability of the thermo-mechanical compensation model of the milling center. 2021. Avaible online: https://stc.fs.cvut.cz/pdf21/11525.pdf?_=1619567509

[45] LJUNG, Lennart. System Identification Toolbox for use with MATLAB. 2011.

[46] HOREJŠ, Otakar, Martin MARES a Jan HORNYCH. A GENERAL APPROACH TO THERMAL ERROR MODELLING OF MACHINE TOOLS. In: 2014.

[47] MAREŠ, Martin. Modelování teplotně mechanických systémů frekvenčními přenosovými funkcemi. Praha: České vysoké učení technické, 2014.

[48] Ljung, L. System Identification Toolbox™ User's Guide. The MathWorks, 2021. https://ch.mathworks.com/help/pdf_doc/ident/ident_ug.pdf

List of figures

List of tables

List of annexes

Text annexes

Annex 1 – LTI response tests and calibration coefficients of the identified transfer functions

Annex 2 – The graphical part of evaluation portability of the thermal errors compensation model set up on target machine 138

Electronic annexes

Michal_Straka_Thesis.pdf

Czech Technical University in Prague

FACULTY OF MECHANICAL ENGINEERING

Department of Production Machines and Equipment

Master's thesis

Influence of input parameters on approximation quality of milling centre thermal error model

Text annexes

2021 **Bc. Michal Straka**

Annex 1

LTI response tests and calibration coefficients of the identified transfer functions

Table: Coefficients (a_n) of the identified transfer functions describing Y and Z axis movement influence on the thermal error in the X, Y, Z directions of MT.

transfer function	a_n coefficient of transfer functions [µm²/°C]			
	a_0	a_1	a_2	a_3
ε_{syst}^{XTY}	0.467234945	-0.467209914	0	0
ε_{stat}^{XTY}	2.350162704	-4.699029841	2.348867151	0
ε_{dyn}^{XTY}	2.990867540	-4.119547491	-0.728143820	1.856823770
ε_{syst}^{XTZ}	0.164570549	-0.316986250	0.152416605	0
ε_{stat}^{XTZ}	1.996092531	-1.996036031	0	0
ε_{dyn}^{XTZ}	3.645066568	-3.645094161	0	0
ε_{syst}^{YTY}	-0.264361275	0.264397691	0	0
ε_{stat}^{YTY}	-0.950216422	1.900341263	-0.950124818	0
ε_{dyn}^{YTY}	-0.594271834	0.594340515	0	0
ε_{syst}^{YTZ}	0.491388911	0.054116609	-0.545454296	0
ε_{stat}^{YTZ}	1.650545105	-1.650450704	0	0
ε_{dyn}^{YTZ}	0.002865645	-0.002865518	0	0
ε_{syst}^{ZTY}	-0.279098394	0.279230573	0	0
ε_{stat}^{ZTY}	-0.552568216	0.552765918	0	0
ε_{dyn}^{ZTY}	-0.715231622	0.715469368	0	0
ε_{syst}^{ZTZ}	-1.213933006	1.213754038	0	0
ε_{stat}^{ZTZ}	-0.076699928	0.153322807	-0.076622900	0
ε_{dyn}^{ZTZ}	-11.882078799	31.941525907	-28.239437213	8.179989188
ε_{amb}	-1.039701172	1.022109354	-1.091116374	1.108640174

Table: Coefficients (b_m) of the identified transfer functions describing Y and Z axis movement influence on the thermal error in the X, Y, Z directions of MT.

transfer function	b_m coefficient of transfer functions [µm]				
	b_0	b_1	b_2	b_3	b_4
ε_{syst}^{XTY}	1	-0.999863728	0	0	0
ε_{stat}^{XTY}	1	-1.644497476	0.291495051	0.353002514	0
ε_{dyn}^{XTY}	1	-0.689710930	-0.984937403	0.046436696	0.628211792
ε_{syst}^{XTZ}	1	-1.990646559	0.990647498	0	0
ε_{stat}^{XTZ}	1	-0.999952847	0	0	0
ε_{dyn}^{XTZ}	1	-0.195044175	-0.804955647	0	0
ε_{syst}^{YTY}	1	-0.999840069	0	0	0
ε_{stat}^{YTY}	1	-1.999227211	0.999227271	0	0
ε_{dyn}^{YTY}	1	-0.999860161	0	0	0
ε_{syst}^{YTZ}	1	-0.999984550	0	0	0
ε_{stat}^{YTZ}	1	-0.999975327	0	0	0
ε_{dyn}^{YTZ}	1	-1.998517447	0.998517475	0	0
ε_{syst}^{ZTY}	1	-0.999863226	0	0	0
ε_{stat}^{ZTY}	1	-0.999873265	0	0	0
ε_{dyn}^{ZTY}	1	-0.999908838	0	0	0
ε_{syst}^{ZTZ}	1	-0.999900035	0	0	0
ε_{stat}^{ZTZ}	1	-1.995486679	0.001358248	1.983786331	-0.989657891
ε_{dyn}^{ZTZ}	1	-1.998489623	0.998489932	0	0
ε_{amb}	1	-0.999974317	0	0	0

Table: Basic parameters of the developed compensation models with FIT and response test results.

Model	T_{in}	Type	Order	*FIT* [%]	Response test
XTY_{in}	T_{syst}	ARX	1,2	29	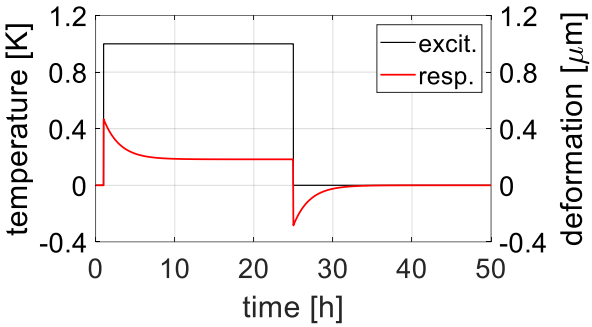 *Fig. Response test for XTY_{syst}.*
	T_{stat}	OE	3,3	73	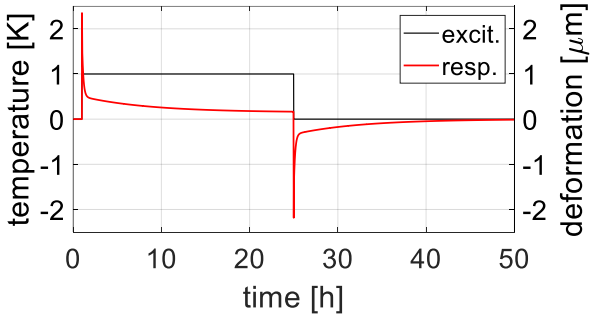 *Fig. Response test for XTY_{stat}.*
	T_{dyn}	OE	4,4	74	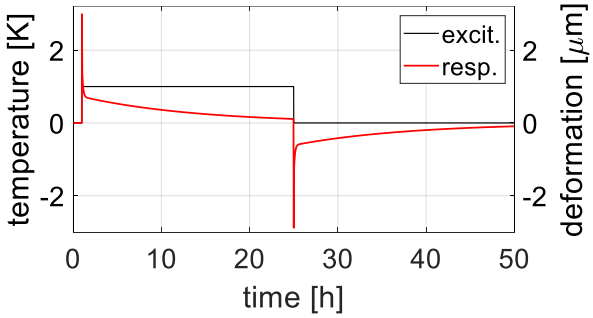 *Fig. Response test for XTY_{dyn}.*
XTZ_{in}	T_{syst}	OE	3,2	91	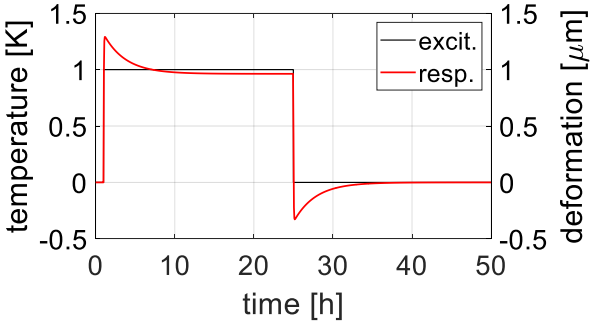 *Fig. Response test for XTZ_{syst}.*

	T_{stat}	OE	2,1	89	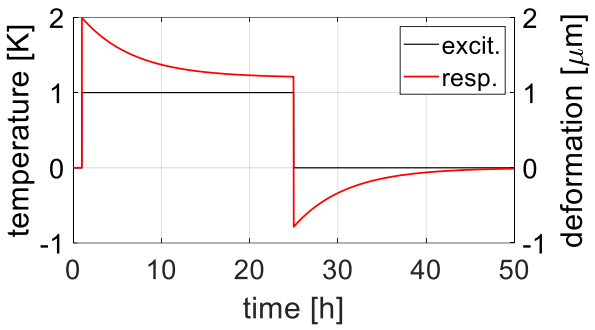 *Fig. Response test for XTZ_{stat}.*
	T_{dyn}	OE	2,2	88	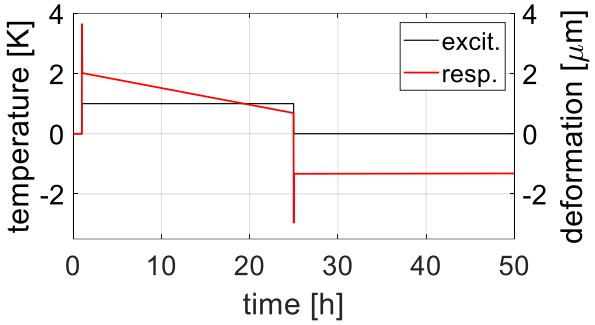 *Fig. Response test for XTZ_{dyn}.*
YTY_{in}	T_{syst}	ARX	1,2	65	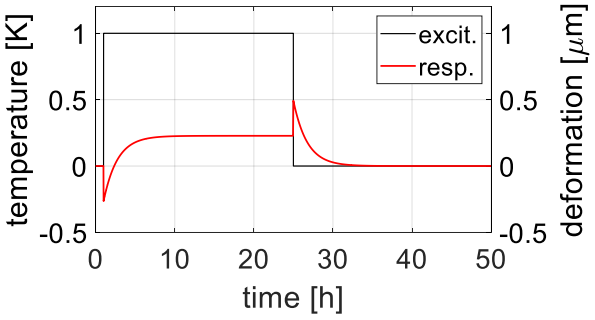 *Fig. Response test for YTY_{syst}.*
	T_{stat}	OE	3,2	76	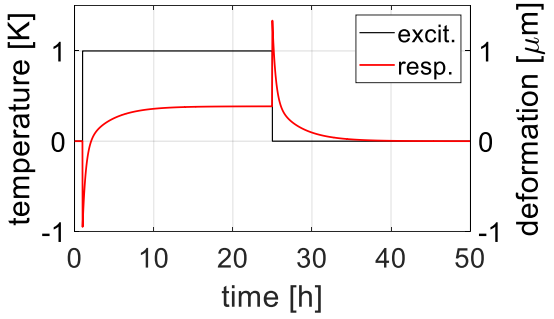 *Fig. Response test for YTY_{stat}.*

	T_{dyn}	ARX	1,2	72	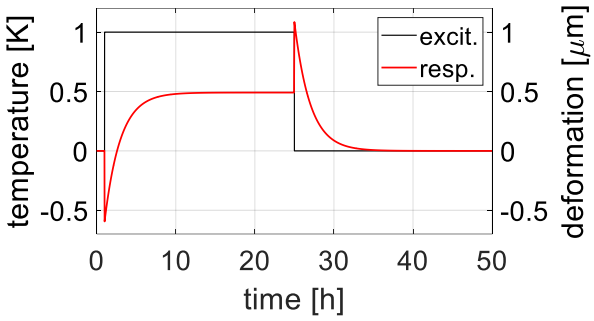 *Fig. Response test for YTY_{dyn}.*
YTZ_{in}	T_{syst}	OE	3,1	92	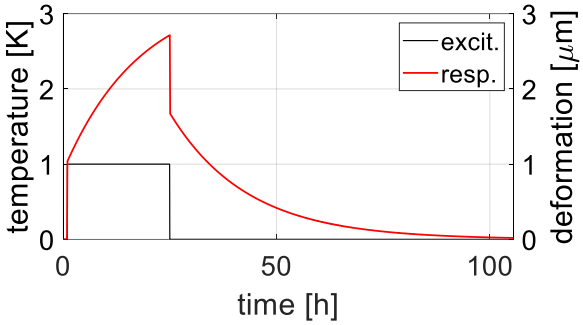 *Fig. Response test for YTZ_{syst}.*
	T_{stat}	OE	2,1	94	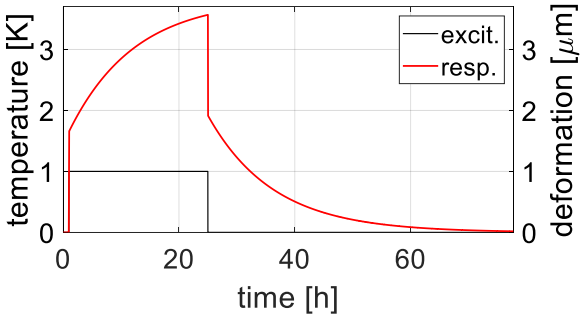 *Fig. Response test for YTZ_{stat}.*
	T_{dyn}	ARX	2,2	97	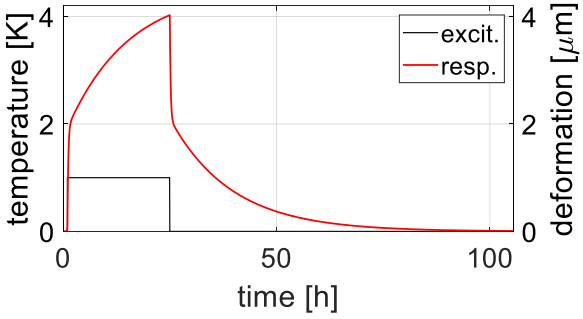 *Fig. Response test for YTZ_{dyn}.*

ZTY_{in}	T_{syst}	ARX	1,2	92	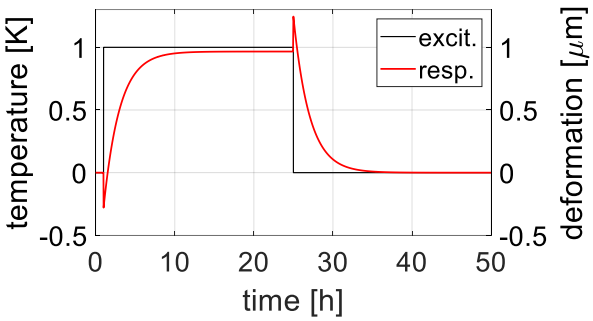 *Fig. Response test for ZTY_{syst}.*
	T_{stat}	ARX	1,2	95	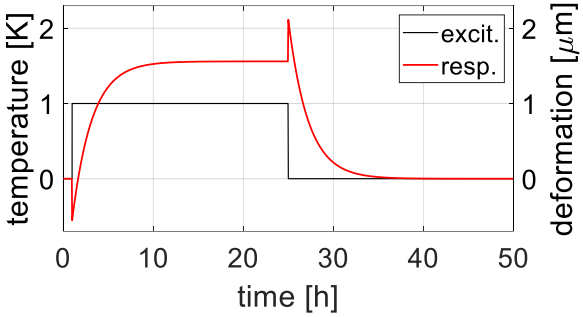 *Fig. Response test for ZTY_{stat}.*
	T_{dyn}	ARX	1,2	95	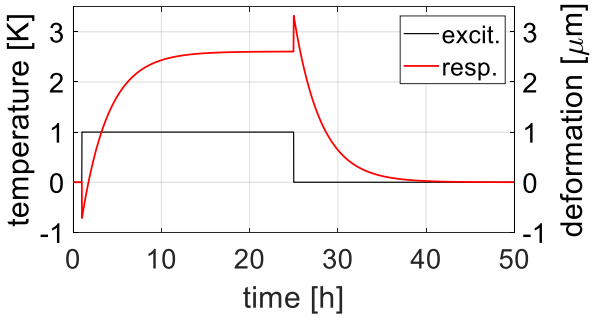 *Fig. Response test for ZTY_{dyn}.*
ZTZ_{in}	T_{syst}	ARX	1,2	93	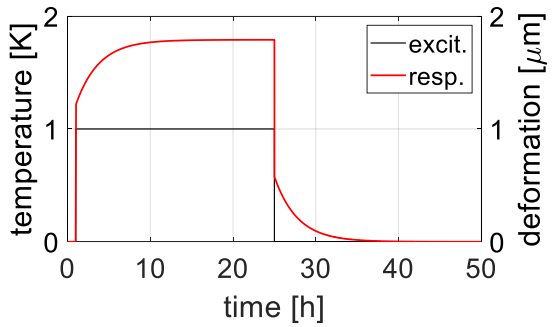 *Fig. Response test for ZTZ_{syst}.*

	T_{stat}	OE	3,4	96	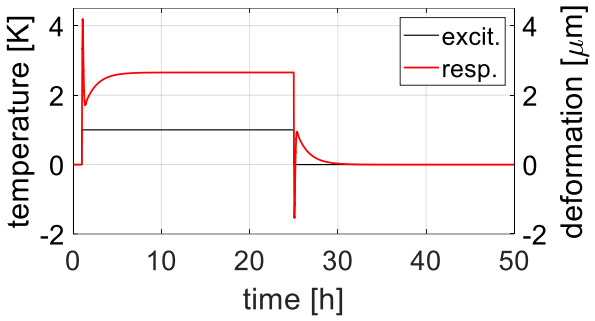 *Fig. Response test for ZTZ_{stat}.*
	T_{dyn}	OE	4,2	97	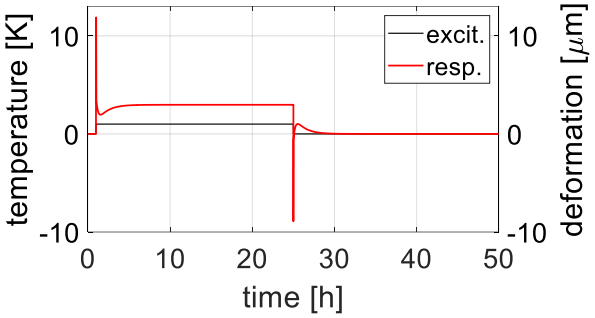 *Fig. Response test for ZTZ_{dyn}.*
Z_{amb}	T_{amb}	ARX	1,4	59	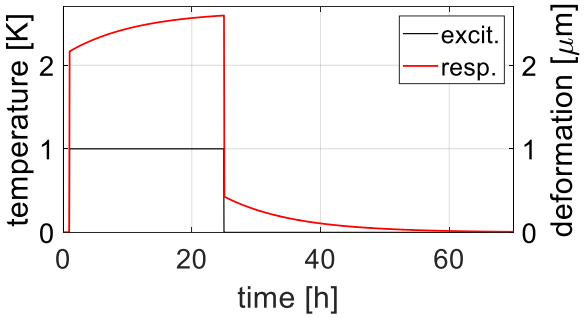 *Fig. Response test for Z_{amb}.*

Annex 2

The graphical part of evaluation portability of the thermal errors compensation model set up on target machine 138

1.1. Results for target machine S/N 118

The uncorrected (by the correction factor) simulated deformation is marked by the left superscript N; see the example of the following equation:

$$ {}^{N}_{138}\mathrm{XTY}_{in}^{S/N} = \Delta T_{in} \cdot \varepsilon_{in}^{XTY} $$

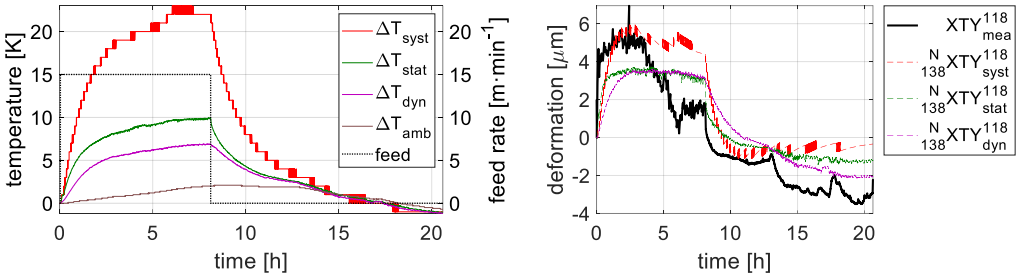

Fig. Behaviours of measured temperatures and Y-axis feed rate (left) and behaviours of measured and simulated deformations in the X direction (right) during test No. 7.

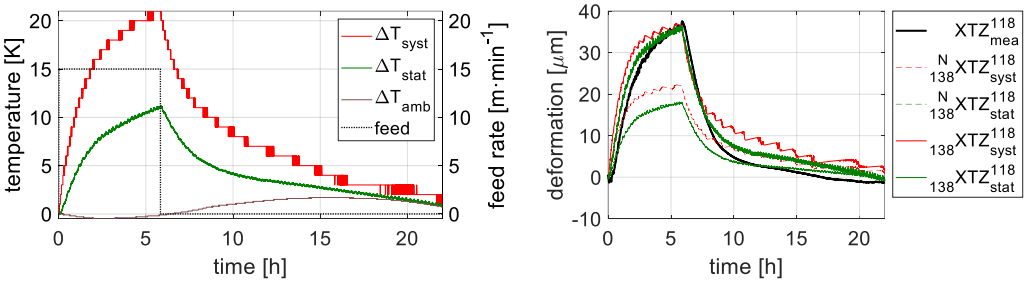

Fig. Behaviours of measured temperatures and Z-axis feed rate (left) and behaviours of measured and simulated deformations in the X direction (right) during test No. 8.

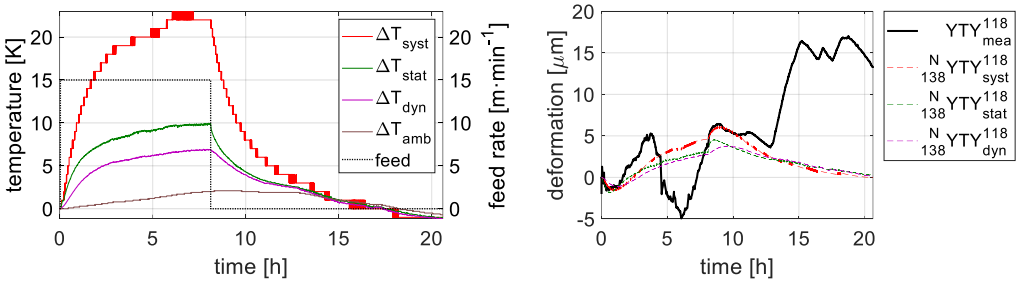

Fig. Behaviours of measured temperatures and Y-axis feed rate (left) and behaviours of measured and simulated deformations in the Y direction (right) during test No. 7.

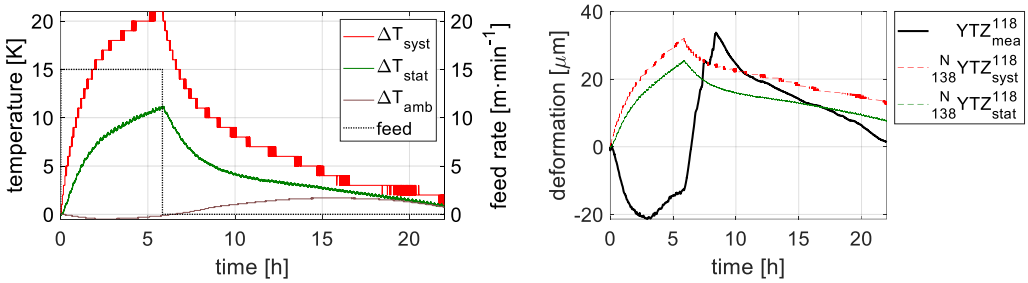

Fig. Behaviours of measured temperatures and Z-axis feed rate (left) and behaviours of measured and simulated deformations in the Y direction (right) during test No. 8.

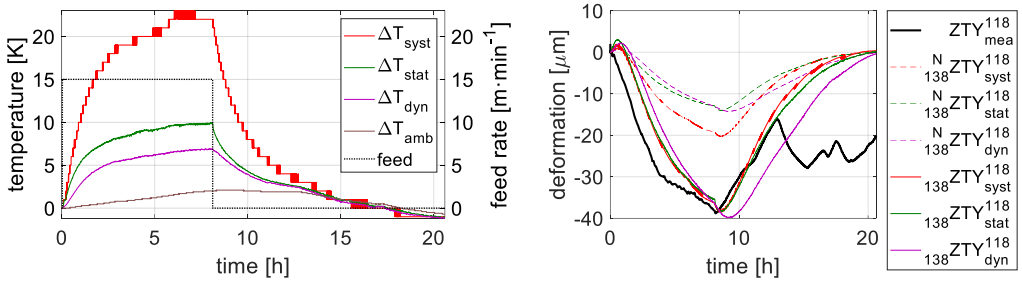

Fig. Behaviours of measured temperatures and Y-axis feed rate (left) and behaviours of measured and simulated deformations in the Z direction (right) during test No. 7.

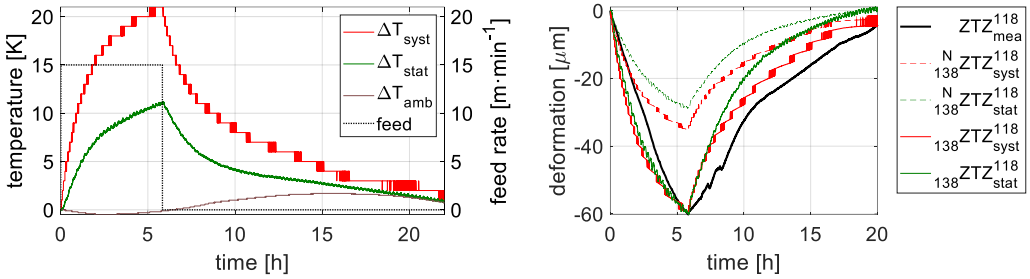

Fig. Behaviours of measured temperatures and Z-axis feed rate (left) and behaviours of measured and simulated deformations in the Z direction (right) during test No. 8.

1.2. Results for target machine S/N 103

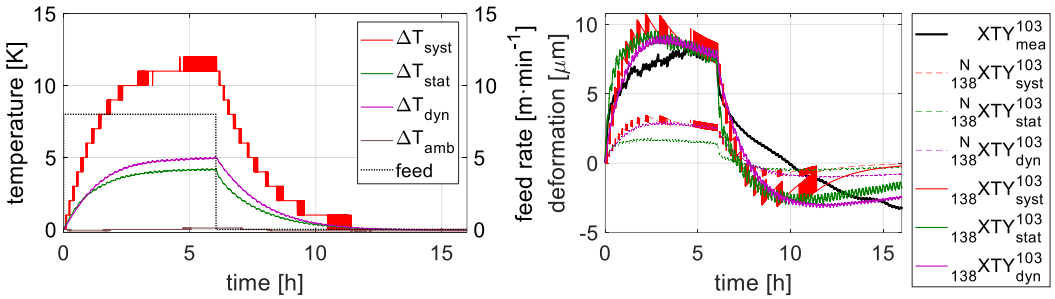

Fig. Behaviours of measured temperatures and Y-axis feed rate (left) and behaviours of measured and simulated deformations in the X direction (right) during test No. 5.

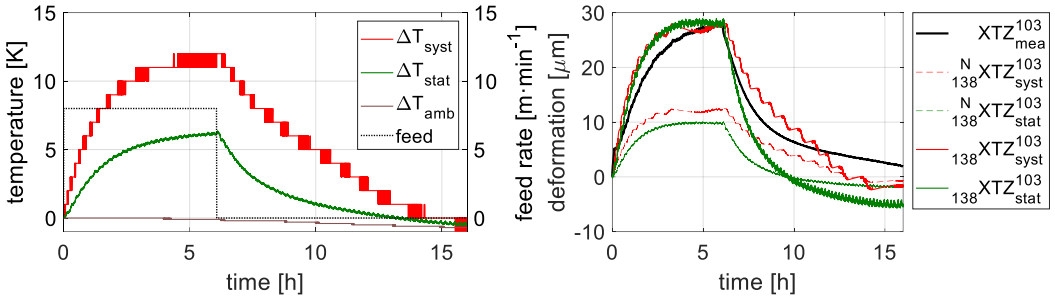

Fig. Behaviours of measured temperatures and Z-axis feed rate (left) and behaviours of measured and simulated deformations in the X direction (right) during test No. 6.

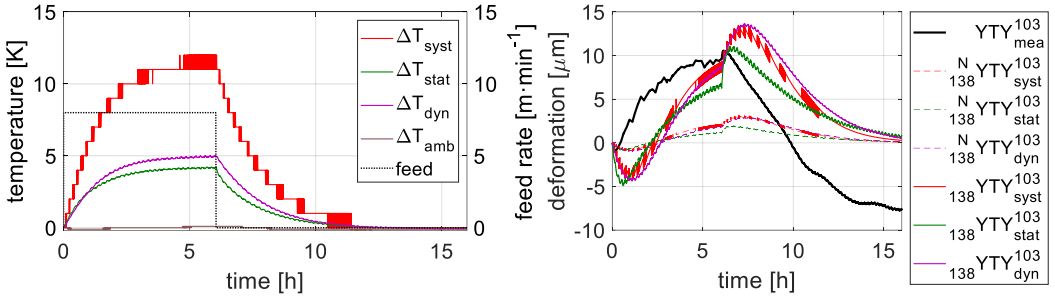

Fig. Behaviours of measured temperatures and Y-axis feed rate (left) and behaviours of measured and simulated deformations in the Y direction (right) during test No. 5.

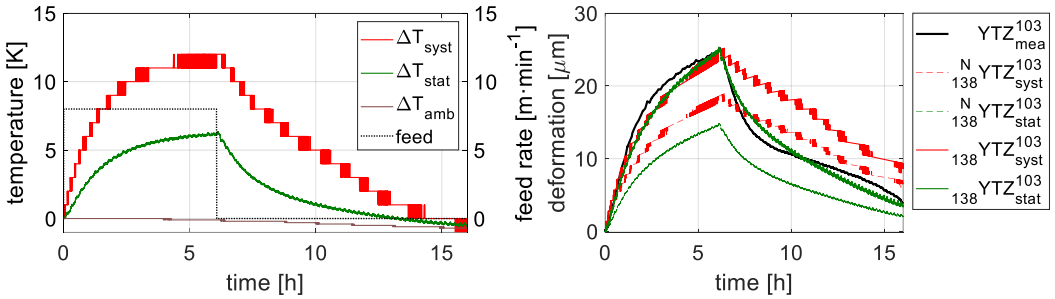

Fig. Behaviours of measured temperatures and Z-axis feed rate (left) and behaviours of measured and simulated deformations in the Y direction (right) during test No. 6.

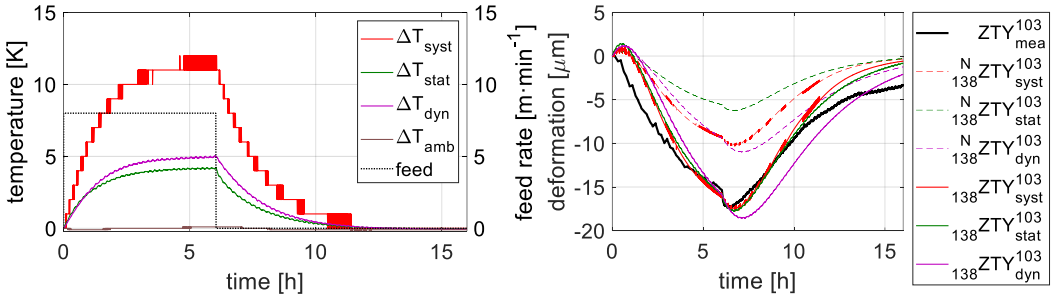

Fig. Behaviours of measured temperatures and Y-axis feed rate (left) and behaviours of measured and simulated deformations in the Z direction (right) during test No. 5.

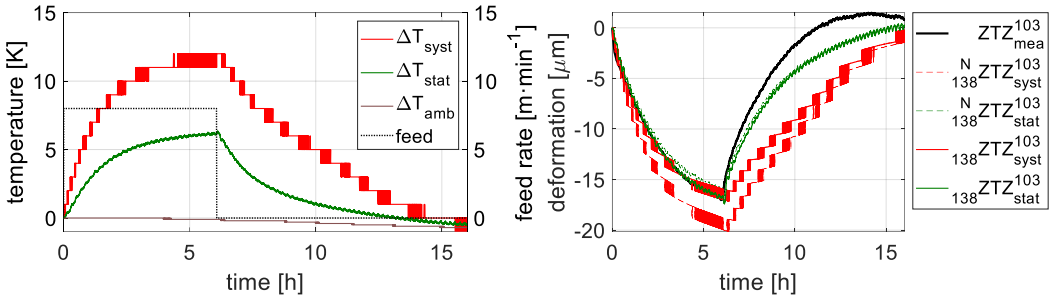

Fig. Behaviours of measured temperatures and Z-axis feed rate (left) and behaviours of measured and simulated deformations in the Z direction (right) during test No. 6.

1.3. Results for target machine S/N 79

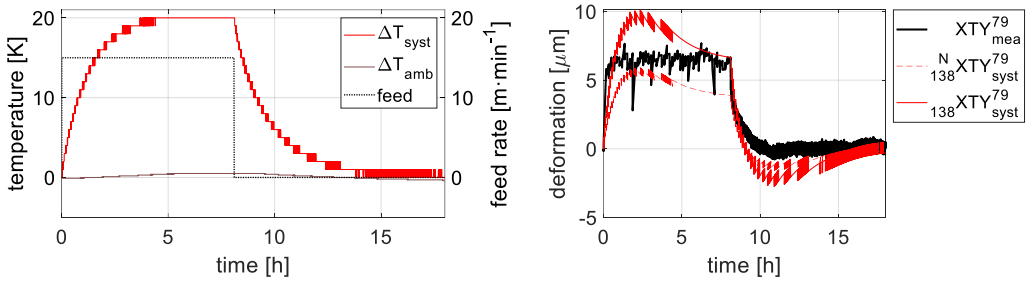

Fig. Behaviours of measured temperatures and Y-axis feed rate (left) and behaviours of measured and simulated deformations in the X direction (right) during test No. 3.

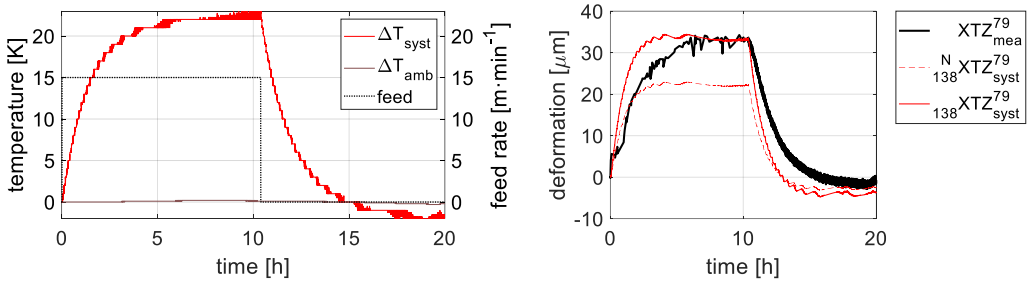

Fig. Behaviours of measured temperatures and Z-axis feed rate (left) and behaviours of measured and simulated deformations in the X direction (right) during test No. 4.

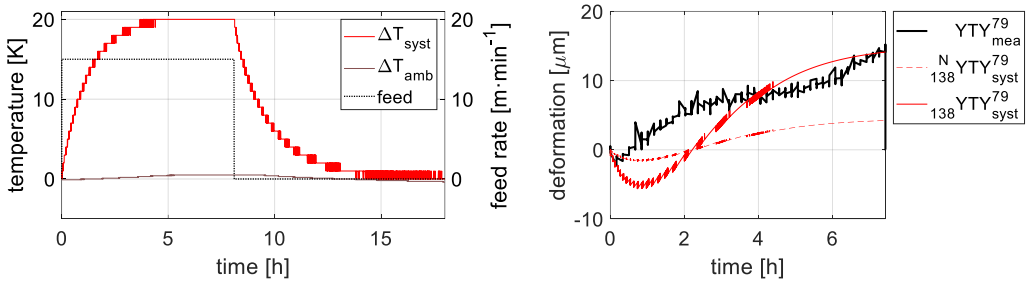

Fig. Behaviours of measured temperatures and Y-axis feed rate (left) and behaviours of measured and simulated deformations in the Y direction (right) during test No. 3.

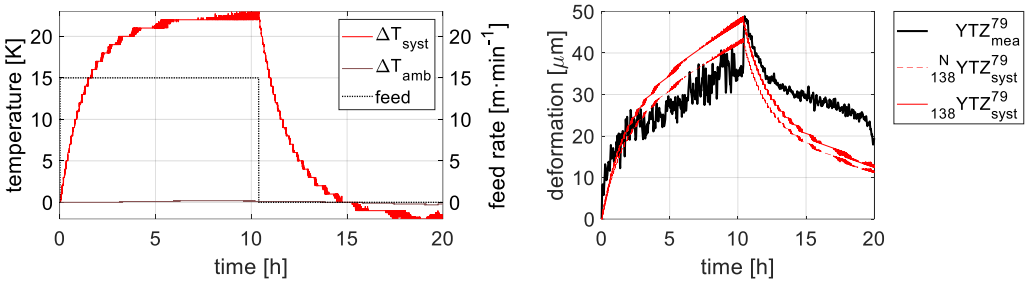

Fig. Behaviours of measured temperatures and Z-axis feed rate (left) and behaviours of measured and simulated deformations in the Y direction (right) during test No. 4.

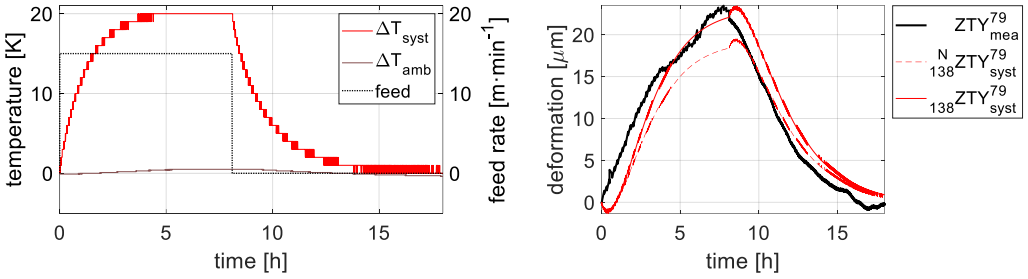

Fig. Behaviours of measured temperatures and Y-axis feed rate (left) and behaviours of measured and simulated deformations in the Z direction (right) during test No. 3.

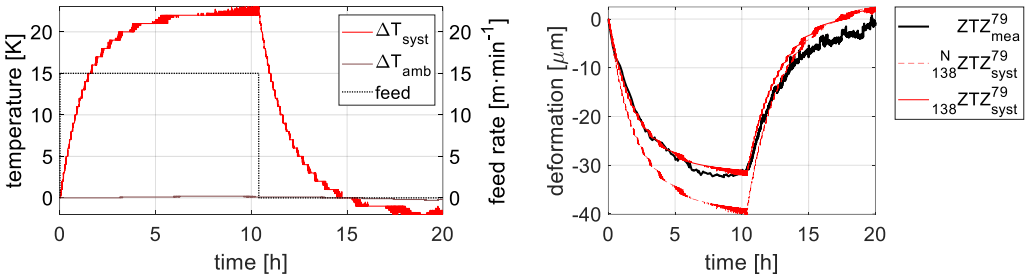

Fig. Behaviours of measured temperatures and Z-axis feed rate (left) and behaviours of measured and simulated deformations in the Z direction (right) during test No. 4.

1.4. Results for target machine AMP

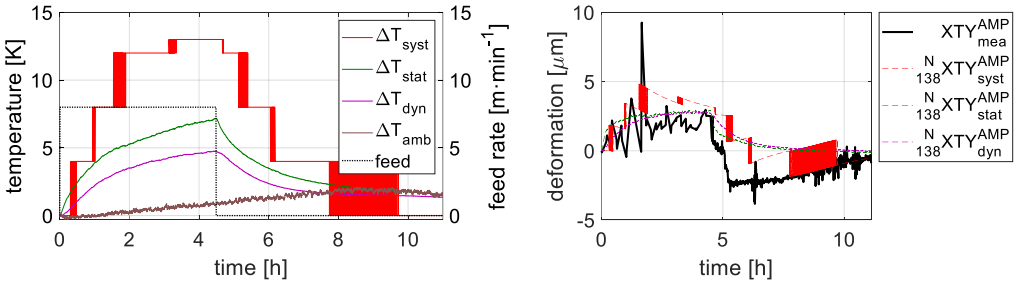

Fig. Behaviours of measured temperatures and X-axis feed rate (left) and behaviours of measured and simulated deformations in the Y direction (right) during test No. 9.

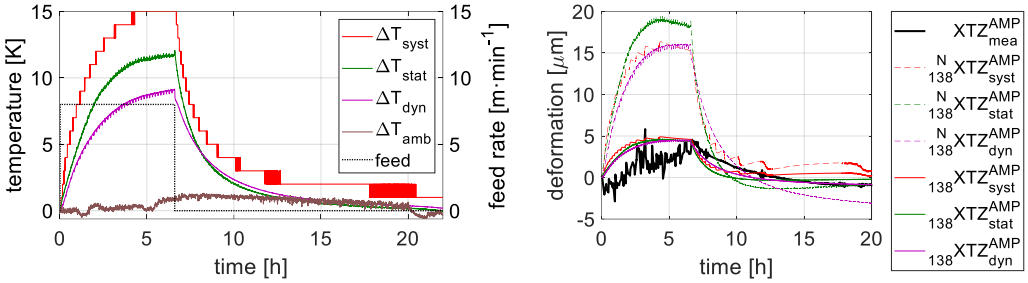

Fig. Behaviours of measured temperatures and X-axis feed rate (left) and behaviours of measured and simulated deformations in the Z direction (right) during test No. 10.

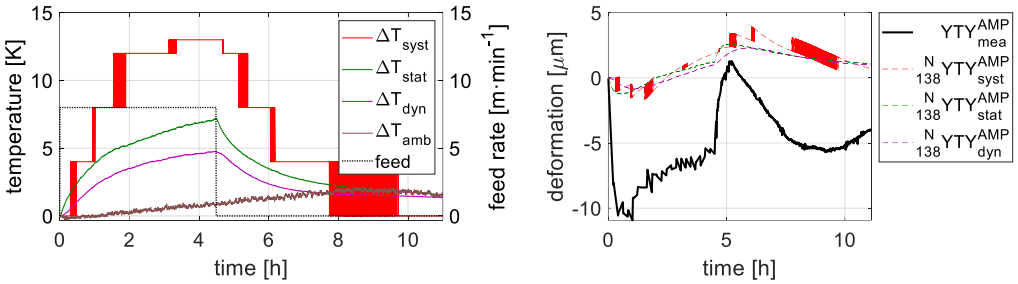

Fig. Behaviours of measured temperatures and Y-axis feed rate (left) and behaviours of measured and simulated deformations in the Y direction (right) during test No. 9.

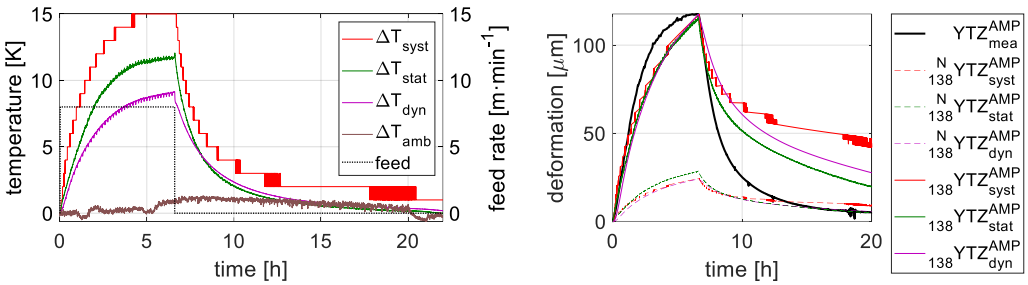

Fig. Behaviours of measured temperatures and Y-axis feed rate (left) and behaviours of measured and simulated deformations in the Z direction (right) during test No. 10.

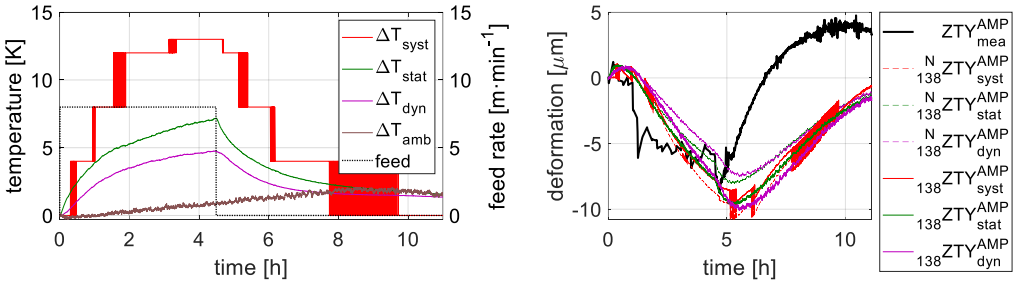

Fig. Behaviours of measured temperatures and Z-axis feed rate (left) and behaviours of measured and simulated deformations in the Y direction (right) during test No. 9.

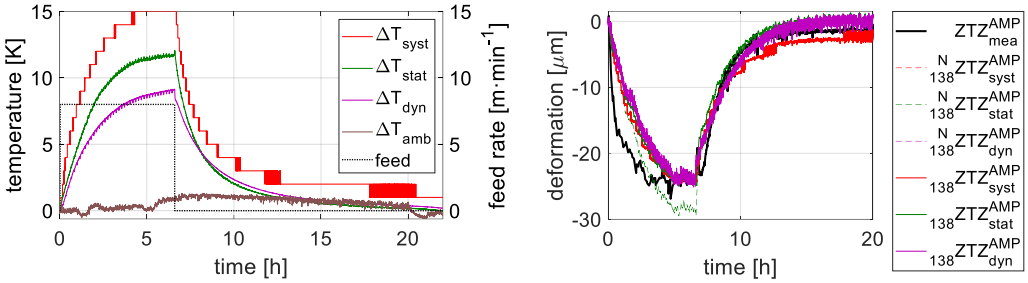

Fig. Behaviours of measured temperatures and Z-axis feed rate (left) and behaviours of measured and simulated deformations in the Z direction (right) during test No. 10.